IAEA-TECDOC-1435

Application of surveillance programme results to reactor pressure vessel integrity assessment

Results of a coordinated research project 2000–2004

IAEA
International Atomic Energy Agency

April 2005

IAEA-TECDOC-1435

Application of surveillance programme results to reactor pressure vessel integrity assessment

Results of a coordinated research project 2000–2004

IAEA
International Atomic Energy Agency

April 2005

The originating Section of this publication in the IAEA was:

Nuclear Power Engineering Section
International Atomic Energy Agency
Wagramer Strasse 5
P.O. Box 100
A-1400 Vienna, Austria

APPLICATION OF SURVEILLANCE PROGRAMME RESULTS TO REACTOR PRESSURE VESSEL INTEGRITY ASSESSMENT
IAEA, VIENNA, 2005
IAEA-TECDOC-1435
ISBN 92–0–101605–0
ISSN 1011–4289

Printed by the IAEA in Austria
April 2005

FOREWORD

This TECDOC has been developed under an IAEA Coordinated Research Project (CRP) on Surveillance Programme Results Application to Reactor Pressure Vessel Integrity Assessment. This CRP is the fifth in a series that have led to the defining of the most appropriate fracture toughness parameters (using relatively small test specimens) for ensuring structural integrity of reactor pressure vessel (RPV) materials.

The CRP group consisted of 20 testing laboratories representing 15 Member States. The CRP had three main objectives: (1) to develop a large database of fracture toughness data using the Master Curve methodology for both precracked Charpy-sized specimens and one-inch thick (25.4 mm) compact tension (1T-CT) specimens, (2) to assess possible specimen bias effects and any effects of the range of temperatures used to determine T_0, either using the single temperature or multi-temperature assessment methods, and (3) to develop international guidelines for measuring and applying Master Curve fracture toughness results for RPV integrity assessment.

Fracture toughness test results showed clear evidence that lower values of unirradiated T_0 were obtained using precracked Charpy specimens compared with results obtained from 1T-CT specimens. This bias in test results is very important when considering the use of precracked Charpy specimens for evaluating RPV integrity. In fact, this is a technical area where the results from this CRP were influential in changing the ASTM test method to include consideration of this effect.

The direct measurement approach using the Master Curve approach for RPV structural integrity assessment has distinct advantages over the indirect methods used in the past for assessing radiation embrittlement effects. The Master Curve methodology already has been or is being assimilated into the ASME Boiler and Pressure Vessel Code, ASTM Standards, USNRC Regulations, German Regulations (KTA 3203), IAEA pressurized thermal shock guidelines for WWER reactors as well as the unified procedure for WWER component lifetime assessment and other industry guidance documents governing RPV integrity analysis.

This report was written to allow nuclear utility engineers and industry scientists to directly measure fracture toughness using small surveillance size specimens of irradiated reactor pressure vessel steels and directly apply the results using the Master Curve approach for RPV structural integrity assessment.

This report provides a summary of Master Curve fracture toughness test results on small surveillance type specimens of the IAEA Reference Material JRQ and other national steels from numerous laboratories throughout the world. Lead contributions were made by the Czech Republic (M. Brumovský), Finland (T. Planman), Germany (H.-W. Viehrig), Hungary (F. Gillemot and M. Horvath), and the USA (W. Server, R. Nanstad and S. Rosinski). W. Server was the chief scientific investigator. The IAEA officers responsible for this publication were V.N. Lyssakov and Ki-Sig Kang of the Division of Nuclear Power.

EDITORIAL NOTE

The use of particular designations of countries or territories does not imply any judgement by the publisher, the IAEA, as to the legal status of such countries or territories, of their authorities and institutions or of the delimitation of their boundaries.

The mention of names of specific companies or products (whether or not indicated as registered) does not imply any intention to infringe proprietary rights, nor should it be construed as an endorsement or recommendation on the part of the IAEA.

CONTENTS

1. INTRODUCTION AND BACKGROUND

The Master Curve approach for assessing fracture toughness of an irradiated reactor pressure vessel (RPV) steel has been gaining acceptance throughout the world. This direct measurement approach is preferred over the correlative and indirect methods used in the past to assess irradiated RPV integrity. Experience in using results obtained from Master Curve testing has been illustrated by Wallin [1], and the approach has been applied utilizing ASTM Standard Test Method E 1921 [2] in the USA [3]. There have been comparisons made using Master Curve data in other countries, but the primary attempts at licensing implementation for nuclear reactor safety of RPVs have been in the USA.

The approach in the USA has been focused on using the Master Curve approach to provide an alternative transition temperature index parameter to be used instead of RT_{NDT}. This new parameter is termed in RT_{T0} [4] and is based on a simple addition of 19.4°C (35°F) to the value of T_0 obtained from ASTM E 1921. This new reference transition temperature can be used to index the existing ASME Code reference toughness curves. The benefit of this approach is that RT_{T0} can be measured directly on irradiated sample materials rather than having to measure initial properties and add transition temperature shift.

This TECDOC summarizes the results generated under the Coordinated Research Project (CRP) “Surveillance Programme Results Application to Reactor Pressure Vessel Integrity Assessment.” The IAEA has sponsored a series of five CRPs that have focused on determining the most appropriate irradiation fracture parameters (using relatively small test specimens) for assuring structural integrity of RPV materials. Some of the background and results from the progression of the CRPs are described next.

The first project (or Phase 1), "Irradiation Embrittlement of Reactor Pressure Vessel Steels", focused on standardization of methods for measuring embrittlement in terms of both mechanical properties and the neutron irradiation environment. Little attention was given at that time (early 1970s) to the direct measurement of irradiated fracture toughness of small surveillance type specimens since elastic–plastic fracture mechanics was in its infancy. The main results from Phase 1, including all reports from participated organizations, were published in 1975 in Report IAEA-176 [5].

Phase 2, "Analysis of the Behaviour of Advanced Reactor Pressure Vessel Steels under Neutron Irradiation", involved testing and evaluation by various countries of so-called advanced RPV steels that had reduced residual compositional elements (copper and phosphorus). Irradiations were conducted to fluence levels beyond expected end-of-life, and the results of Phase 1 were used to guide the overall approach taken during Phase 2.

In addition to transition temperature testing using Charpy V-notch test specimens, some emphasis was placed on using tensile and early-design fracture toughness test specimens applying elastic–plastic fracture mechanics methods. Further progress in the application of fracture mechanics analysis methods for radiation damage assessment was achieved in this phase. Improvement and unification of neutron dosimetry methods provided better data with less inherent scatter. All results together with their analyses and raw data were summarized in IAEA Technical Reports Series No. 265 [6].

The third phase included the direct measurement of fracture toughness using irradiated surveillance specimens. "Optimising Reactor Pressure Vessel Surveillance Programmes and Their Analyses" was the title for Phase 3, and significant accomplishments were achieved

concerning fracture toughness testing and structural integrity methods, correlations between various toughness and strength measures for irradiated materials, emphasis on the need to understand embrittlement mechanisms, and potential mitigative measures for radiation embrittlement.

One key achievement was the acquisition and testing of a series of RPV steels designed and selected for radiation embrittlement research. One of these materials was given the code JRQ, and it has been shown to be an excellent correlation monitor (or standard reference) material as documented in IAEA-TECDOC-1230 [7].

The main emphasis during the fourth phase, which began in 1995, was the experimental verification of the Master Curve approach for surveillance size specimens. This CRP was titled "Assuring Structural Integrity of Reactor Pressure Vessels", and was directed at confirmation of the measurement and interpretation of fracture toughness using the Master Curve method with structural integrity assessment of irradiated RPVs as the ultimate goal. The final report [8] will include a CD with the results of the Phase 3 project.

The main conclusions from the Phase 4 CRP are that the Master Curve approach has demonstrated that small size specimens, such as precracked Charpy, can be used to determine valid values of fracture toughness in the transition temperature region. Application included a large test matrix using the JRQ steel and other national steels including WWER materials. No differences in laboratories were identified, and results from dynamic data also followed the Master Curve.

The Phase 5 CRP is now completed. The large CRP group consisted of 20 testing laboratories representing 15 Member countries. This CRP, “Surveillance Programme Results Application to Reactor Pressure Vessel Integrity Assessment,” had two main objectives:

- Develop a large database of fracture toughness data using the Master Curve methodology for both precracked Charpy size and one-inch thick (25.4 mm) compact tension (1T-CT) specimens to assess possible specimen bias effects and any effects of the range of temperatures used to determine T_0, either using the single temperature or multi-temperature assessment methods.

- Develop international guidelines for measuring and applying Master Curve fracture toughness results for RPV integrity assessment.

Fracture toughness test results show clear evidence that lower values of unirradiated T_0 are obtained using precracked Charpy specimens as compared to results from 1T-CT specimens. This bias in test results is very important when considering use of precracked Charpy specimens in evaluating RPV integrity. In fact, this is a technical area where the results from this CRP were influential in changing the ASTM Test Method to include consideration of this effect. Other key results are presented in this report that formed part of the basis for the TRS, “Guidelines for Application of the Master Curve Approach to Reactor Pressure Vessel Integrity”, which was aimed at application of the Master Curve approach for small surveillance size specimens [9].

Scientists and engineers from Argentina, Brazil, Bulgaria, the Czech Republic (two laboratories), the European Commission (JRC), Finland, France, Germany (two laboratories), Hungary, Japan, the Republic of Korea, Romania, the Russian Federation (two laboratories), Spain, and the United States of America (three laboratories) contributed to the development of

these guidelines. A list of the organizations and key individuals that participated in the CRP is provided in the Appendix.

2. PURPOSE OF THE FIFTH CRP

The focus of the Fifth CRP was on use of the Master Curve approach for assessing structural integrity of RPVs using small surveillance size specimens, such as the precracked Charpy loaded in three-point bending. In order to assess the use of this small specimen, a plan to test a single material by all of the participating laboratories was established, as well as additional testing of national steels and other related characterizations. The material selected for the quasi round robin testing was the IAEA standard reference material JRQ.

JRQ is a special heat of A533B-1 steel fabricated in Japan to show relatively large changes in mechanical properties when exposed to neutron radiation [7]. This heat of steel was tested extensively in this and other CRPs and has been used as an international standard reference material. The test program developed for the fifth CRP focused on two key aspects of Master Curve testing using the JRQ material: (1) multi-temperature testing as allowed in the latest approved version (2002) of ASTM E 1921 [2], and (2) comparison of 10-mm square three-point single-edge bend, SE(B)[1], specimen and 25.4 mm compact tension (1T-CT) specimen test results.

Other aspects of Master Curve results with regard to material homogeneity and data scatter are addressed later in this report. Additional non-mandatory testing at several laboratories also was focused on other RPV steels, use of other test specimen sizes and types, and other evaluations focused to identify either large data scatter and/or material non-homogeneity.

This TECDOC has been written to allow nuclear utility engineers and industry scientists to directly measure fracture toughness using small surveillance size specimens of irradiated reactor pressure vessel steels and directly apply the results using the Master Curve approach for RPV structural integrity assessment. This direct measurement approach has distinct advantages over the indirect methods used in the past for assessing radiation embrittlement effects. The Master Curve methodology already has been or is being assimilated into the ASME Boiler and Pressure Vessel Code, ASTM Standards, USNRC Regulations, German Regulations (KTA 3203), IAEA PTS Guidelines for WWER reactors as well as the VERLIFE procedure “Unified Procedure for WWER Component Lifetime Assessment” and other industry guidance documents governing RPV integrity analysis.

[1] This specimen type is often referred to as a precracked Charpy specimen since it is the equivalent of a Charpy type specimen with a fatigue crack instead of a shallow machined V-notch to allow it to be tested as a fracture toughness specimen.

3. CONTRIBUTIONS OF INDIVIDUAL ORGANIZATIONS

The countries and organizations involved in the testing for the fifth CRP are identified in Table 3.1. The designation code for each participating organization is also indicated along with the type of specimen(s) and material(s) tested. Further details on the actual test matrices for the JRQ steel and the analysis of the test results are contained in Sections 5 and 7, respectively. Results from the additional testing of the national steels are presented in Sections 5 and 8. Other characterization testing for JRQ and national steels also is covered in Section 9. All of the individual laboratories and key participants involved in this CRP are identified in the Appendix.

Table 3.1 – Countries/Organizations Participating in the Fifth CRP and Final Contributions

Country	Organization	Code	JRQ Tests		National Steel(s) Tested	Other Tests
			10-mm square SE(B)	1T-CT		
Argentina	Comisión Nacional de Energía Atómica	ARG	Yes	No	Yes	No
Brazil	CNEN/CDTN	BRA	Yes	No	Yes	No
Bulgaria	Institute of Metal Science	BUL	Yes	No	No	No
Czech Republic	Nuclear Research Institute	NRI	Yes	Yes	No	Yes
Czech Republic	Vitkovice Research and Development	VIT	Yes	Yes	Yes	No
Finland	VTT Industrial Systems	FIN	Yes	No	Yes	Yes
Germany	Forschungszentrum Rossendorf e.	IWM	Yes	Yes	No	No
Germany	Fraunhoffer Institute fuer Werkstoffmechanik	FZR	Yes	Yes	No	Yes
Hungary	Atomic Energy Research Institute	HUN	Yes	No	Yes	No
Japan	Japan Atomic Energy Research Institute	JAP	Yes	No	No	No
Korea, Rep. of	Korea Atomic Energy Research Institute	KOR	Yes	No	Yes	Yes
Romania	Metallurgical Research Institute	ROM	Yes	Yes	Yes	No
Russian Federation	RRC “Kurchatov Institute”	KUR	Yes	No	Yes	No
Russian Federation	Prometey Institute	PRO	Yes	Yes	Yes	No
Spain	CIEMAT	ESP	Yes	No	Yes	Yes
USA	EPRI	USE	Yes	No	Yes	No
USA	ATI	USI	Yes	No	Yes	Yes
USA	Oak Ridge National Laboratory	USO	Yes	Yes	Yes	Yes

4. INTERNATIONAL DATABASE OF REACTOR PRESSURE MATERIALS FOR THE MASTER CURVE EVALUATION

A programme on Lifetime Management of Nuclear Power Plants (LMNPP) has been promulgated by the IAEA to facilitate the international exchange of information on the behaviour of key components. Another programme on the reliability of NPP pressurised components has been established under the aegis of the Technical Working Group on the LMNPP (TWG-LMNPP). It has been proposed by the TWG-LMNPP that the IAEA should expand that activity and put forward a proposal for the development of an "International Database on NPP Life Management" [10]. A decision was made to build the database step by step on a modular basis. The first module was designed for the examination of irradiation effects, and it involved collection of both utility surveillance and research data. The database has also added a module to collect the fracture toughness and other characterization data from the Fifth and previous CRPs.

A short summary of the RPV material section of the IAEA International Database on Reactor Pressure Vessel Materials (IDRPVM) [11] is discussed next. One of the main goals of the database is to assist researchers in understanding underlying trends, identifying potential mechanisms, and storing valuable data for future studies. The database management organization includes the following:

- *IAEA* organizes the database according to requests from Member States.
- *Custodians* act as the agent for the IAEA in operating and maintaining the database and providing an effective interface for Member States and participating organizations. The Custodian also performs data acquisition from Member States and database members and assists with data evaluation and distribution, as appropriate.
- *Steering Committee* supervises the data flow and database use.
- *Database Members* are the persons or organizations from Member States that provide and are entitled to use the database, as well as to receive database information. Each Database Member is responsible for data acquisition, data validation, and final verification. All Database Members must adhere to the strict observation of the database rules.

Fourteen countries have supplied large quantities of surveillance data, greatly enlarging the surveillance section. Results from some large IAEA research programmes also have been added to the database research section:

- CRP Phase 3, "Optimizing of Reactor Pressure Vessel Surveillance Programmes and their Analysis"
- CRP Phase 4, "Assuring Structural Integrity of Reactor Pressure Vessels"
- CRP Phase 5, "Surveillance Programme Results Application to Reactor Pressure Vessel Integrity Assessment"
- Round-Robin Tests on "WWER-440 Weldments".

Recently the shared costs for coordinating nuclear research projects through the European Union (EU) Fifth Framework Programme were discussed, and the research section of the database was made available to the Joint Research Center (JRC) of the EU, Institute for Energy, Petten, Netherlands. JRC became a Database Member.

Some of the key features of the database are:

- The database can include not only data (raw data are collected) but also store visual information (diagrams and metallography pictures).
- The software chosen for the database is MS Access to make the database user friendly and to provide a common system for the participants. All data are stored in Access format, but data export can be accomplished in several different formats.
- About 15 000 Charpy V-notch, 3000 tensile, 4000 fracture toughness data (mostly measured on irradiated RPV steels) are included in the database. A large number of other related characterization data also are contained in the database, and the quantity is continuously increasing.
- The database includes a large variety of RPV steels and model alloys.

The following actions relative to the database are currently ongoing:

- Collection of additional data from participants who have already joined or from others who are preparing their membership application and have not yet supplied data.
- Incorporation of new members once negotiations are completed involving several countries.
- Organising more intensive use of the database; one new CRP is being pursued on "Evaluation of Radiation Damage of WWER Reactor Pressure Vessel using IAEA Database on Reactor Pressure Vessel Materials."

The Master Curve methodology is a relatively new development in the fracture mechanics community. At the foundation of the database are different dataset needs for fracture toughness data storage. Therefore, the Static Fracture Toughness portion of the database had to be extended with the several new fields: $J_{elastic}$ (J-integral elastic contribution); $J_{plastic}$ (J-integral plastic contribution); CALCMETHOD (selection of ASTM E 1921Test Methods used [2]); J_c; K_{jc}; $K_{jclimit}$; CENSORED; $K_{jc(1T)}$, $T_{0(single)}$; $T_{0(multi)}$ (Characteristics according to ASTM 1921); and Loading type (tension, three point bending etc.). More than 1,500 fracture mechanics test results obtained on the JRQ material are in the database. These data have been stored in the database for the current analysis of the project results and for further evaluations in future projects.

5. TESTED MATERIALS (JRQ AND NATIONAL STEELS)

5.1. IAEA REFERENCE RPV STEEL JRQ

The IAEA reference RPV steel, Japanese reference quality (JRQ), was selected for the mandatory part of the CRP for RPV model steel. It was made by Japan steel works, and had on purpose a known sensitivity to neutron irradiation. The composition was C: 0.18%, Si:0.24%, Mn: 1.42%, P: 0.017%, S: 0.004%, Cu: 0.14%, Ni: 0.84%, Cr: 0.12%, Mo 0.51%, V: 0.002%, Al: 0.014%. This is a model alloy similar to A533B RPV steel but the impurity copper was added on purpose to ensure high sensitivity to neutron embrittlement.

JRQ is ASTM A 533 grade B class 1 steel to show relatively large changes in mechanism properties when exposed to neutron radiation. This steel has been extensively tested and characterized in different IAEA and other international research programs.

A description of the manufacturing history and an overview of material preparation for testing, subsequent acceptance testing results, and results obtained during IAEA CRPs have been documented by Brumovsky [7]. The microstructure of the 225 mm thick JRQ plate varies through the thickness. In Figure 5.1, the microstructure at the surface and within the middle section of the plate is depicted. The microstructure is mainly bainitic. At the surface there are both lower bainite and martensite. In the middle region heterogeneously composed upper bainite together with reticularly arranged martensite are visible. The reticularly arranged martensitic structure becomes more pronounced with the distance from the surface and could be explained by segregation [12]. The hardness of the reticularly arranged martensitic structure is about 25% higher than the hardness of the matrix. The segregations were analyzed by X ray spectroscopy (energy dispersive) and ion-beam. In summary the segregations show higher concentrations in Cr (+15%), Mn (+23%), Cu (+20%) and Mo (+30%) contents compared with the matrix [13].

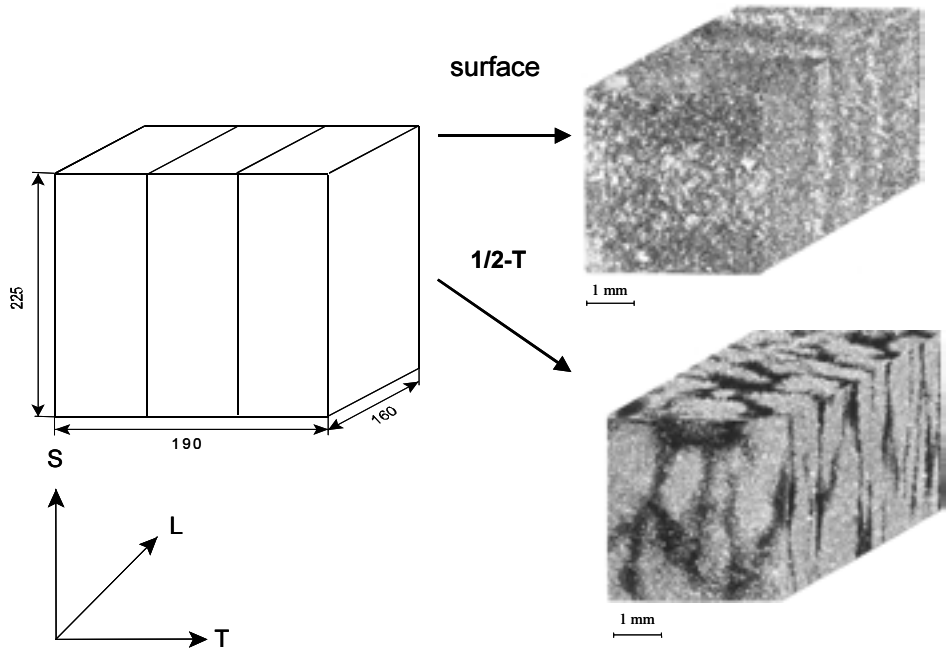

FIG. 5.1 – Microstructure at the Surface and Within the Middle Section of 5JRQ Steel Plate (Block 5JRQ22).

Figure 5.2 shows the dependence of the Charpy-V ductile-to-brittle transition temperature, T_{41J}, and Master Curve reference temperature, T_0, on the thickness of JRQ plate 5JRQ22 investigated within a former IAEA CRP [12]. Obviously, the Charpy-V T_{41J} and T_0 values increase by about 55 K from the surface to the middle of the plate. Both parameters show the same trend with strong scatter at different thickness locations, especially within the middle range. This scatter is due to the inhomogeneous structure within the middle range of the plate. Within the ¼- to the ¾-thickness region, the following mean ductile-to-brittle transition temperature parameters were determined:

Charpy T_{41J}: –20°C ±11.4 K
Master Curve T_0: –70°C±6.5 K

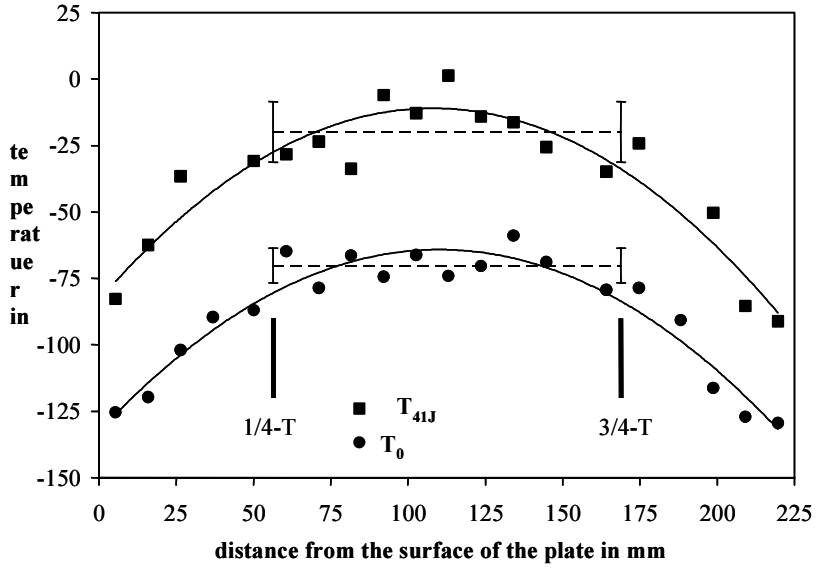

FIG. 5.2 – Charpy T_{41J} and T_0 versus Distance from the Surface in the 5JRQ Steel Plate (Block 5JRQ22).

The trend for the Charpy-V T_{41J} and Master Curve T_0, as shown in Figure 5.2, can be interpreted as an increase in the transition temperature with thickness from either surface and then remaining constant within ¼- to the ¾-thickness region with a fair amount of data scatter.

Taking into account this gradient of the mechanical properties, the specimens for the mandatory part of this CRP were stipulated to be machined from ¼- and ¾-thickness location (¼-T, ¾-T) of the specific JRQ plate. The JRQ test blocks distributed to the different laboratories were mainly from test plate 6JRQ [7]. Figure 5.3 depicts the sampling scheme of plate 6JRQ. However, some laboratories tested JRQ specimens from test plates 5JRQ and 3JRQ used in previous IAEA CRPs. The predominant specimen types tested were precracked Charpy size single edge bend, SE(B), specimens and 25.4 mm (one-inch thick) thick compact tension (1T-CT) specimens in the transverse (TL) orientation according to ASTM Standard Test Method E399 [14].

Figure 5.4 depicts the cutting scheme and the microstructures in the ¼-T and ½-T location of block 6JRQ12 investigated by FZR (Germany) as a typical example. No difference in the structure can be seen between the two thickness locations. The specific JRQ blocks and final specimen test matrices for the countries and laboratories are shown in Tables 5.1 and 5.2 for the Charpy size SE(B) and 1T-CT specimens, respectively. As identified in Tables 5.3, and 5.4, some additional tests of 1T-CT and SE(B) specimens were performed at the ½-T location of the plate. Additionally, a few optional specimens of different geometries, orientations, and JRQ blocks were tested (see Table 5.5). Limited irradiations were carried out by Ciemat, Spain (ESP) as indicated in Table 5.6. Further details on other additional testing that was performed are provided in Section 9.

6JRQ11* FIN	**6JRQ12* FZR**	**6JRQ13* USO**	**6JRQ14* VIT**
6JRQ21* FIN	**6JRQ22* ROM**	**6JRQ23* NRI**	**6JRQ24***
6JRQ31 BRA**	**6JRQ32** HUN**	**6JRQ33** HUN**	**6JRQ34** ESP**
6JRQ41**	**6JRQ42** BUL**	**6JRQ43** IWM**	**6JRQ44** PRO**
6JRQ51 JAP**	**6JRQ52****	**6JRQ53****	**6JRQ54****

* block dimension: 208 mm × 242 mm × 225 mm
** block dimension: 185 mm × 242 mm × 225 mm

FIG. 5.3 – Sampling Scheme of Plate 6JRQ.

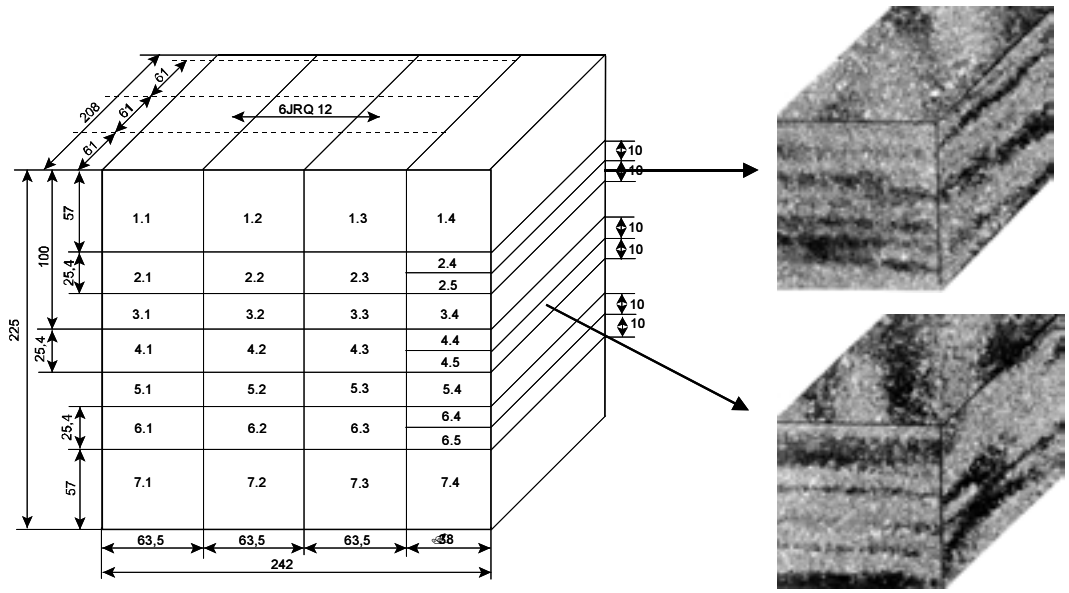

FIG. 5.4 – Cutting Scheme and Metallographic Structure of Block 6JRQ12.

Table 5.1 – Test Matrix for SE(B) Tests from the ¼-T and ¾-T Locations

Code	JRQ Block	Number of Specimens at Test Temperature										
		-110°C	-100°C	-90°C	-85°C	-80°C	-75°C	-70°C	-60°C	-50°C	-40°C	Total
ARG	3JRQ11					3		4	3	4		14
BRA	6JRQ31		4	7		3		5	5			24
BUL	5JRQ54	3	6	6								15
NRI	6JRQ23	3		6		4		5	5			23
VIT	6JRQ14					6		6	3	3		18
FIN	6JRQ21		6	6					6			18
FZR	6JRQ12	3		6		3			3			15
IWM	6JRQ43							1	1	6	1	9
HUN	6JRQ33	8		8	1			8	8			32
JAP	6JRQ51	6		6						8		20
KOR	5JRQ25		8	8		9	8	10	10			53
ROM	6JRQ22		3	6					3			12
KUR	5JRQ33				11	6		6	3			26
PRO	6JRQ44	7		8		8		6				29
ESP	6JRQ36		6	6					6			18
USE	5JRQ45			6		7		4				17
USI)	5JRQ45		5	6		3		8				22
USO	6JRQ13	6		6					6			18
Total		36	38	91	12	52	8	63	62	21	1	383

Table 5.2 – Test Matrix for 1T-CT Tests from the ¼-T and ¾-T Locations

Code	JRQ Block	Number of Specimens at Test Temperature									
		-140°C	-100°C	-90°C	-85°C	-70°C	-50°C	-40°C	-30°C	-20°C	-10°C	Total
NRI	6JRQ23					15						15
VIT	6JRQ14						2		4	2	1	9
FZR	6JRQ12			3		6				3		12
IWM	6JRQ43	1	1		1	1	1[a]	1		1[b]	8	15
ROM	6JRQ22					3	6			3		12
PRO	6JRQ44						8					8
USO	6JRQ13			6					6			12
Total		1	1	9	1	25	17	1	12	9	10	83

[a] Tested at –55°C.
[b] Tested at –25°C.

Table 5.3 – Test Matrix for SE(B) Tests from the ½-T Location

Code	JRQ Block	Number of Specimens at Test Temperature					
		-100°C	-90°C	-80°C	-70°C	-60°C	Total
VTT	6JRQ21	3	3			3	9
FZR	6JRQ12			3	3	3	9
USO	6JRQ13		6				6
Total		3	9	3	3	6	24

Table 5.4 – Test Matrix for 1T-CT Tests from the ½-T Location

Code	JRQ Block	Number of Specimens at Test Temperature				
		-70	-50	-40	-30°C	Total
NRI	6JRQ23	9				9
FZR	6JRQ12		3		3	6
USO	6JRQ13			9		9
Total		9	3	9	3	24

Table 5.5 – Test Matrix for the Optional Portion on Unirradiated JRQ

Code	JRQ Block	Thickness (mm)	Number of Specimens at Test Temperature						Specimen Type and Orientation
			-140°C	-95°C	-80°C	-70°C	-60°C	Total	
BRA	5JRQ55	45		9				9	SE(B), TL
ESP	6JRQ34	56			19	2	8	29	SE(B), TS

Note: Ciemat (ESP) tested irradiated specimens of block 3JRQT71 and 3JRQT76 (see Table 5.6).

Table 5.6 – Test Matrix for Optional Portion, Irradiated Specimens of JRQ
(Fluence = 3.64×10^{22} m^{-2} (E >1 MeV) at an Irradiation Temperature of 290°C)

Code	JRQ Block	Number of Specimens at Test Temperature						Specimen Type and Orientation
		-50°C	-40°C	-30°C	-20°C	-10°C	Total	
ESP	3JRQT71	2	4	6	8	2	22	SE(B), TL
ESP	3JRQT76			2	2	1	5	0.5T-CT, TL

5.2. NATIONAL STEELS

Some specific materials were re-evaluated from the extensive amount of national steels included in the CRP. Note that the main emphasis in the testing portion of the CRP was focused on the JRQ steel, and only selected national steels were re-evaluated. The test matrices for the countries and laboratories for whom national materials were re-evlauated are shown in Table 5.7. Note that both Charpy size SE(B) and 1T-CT specimens were tested to assess any differences between the two specimen types and sizes. Further details on other additional testing that was performed on the national steels are provided in Section 9.

Table 5.7 – Test Matrix for Some of the Optional Portion for National Materials

Code	Type of Material	Material Code	Location in Thickness (mm)	Specimen Type	Orientation	V_0 (mm/min)	Total Tests
BRA	22 MnNiMo 5 5			SE(B)	LS	0.2	25
ESP	A533B-1	1MVE5	43	SE(B)	TL	0.15	19
ESP	A533B-1	1MVE5	55	SE(B)	TL	300	17
ESP	A533B-1	2MVE51MVE. U1	43–74	1T-CT	TL	0.15	23
ESP	A533B-1	JPJ24	68	SE(B)	TL	0.15	18
JAP	A533B	Steel A	67	SE(B)	TL	0.2	10
JAP	A533B	Steel B	63	SE(B)	TL	0.2	10
JAP	A533B	Steel A	63	1T-CT	TL	0.5	24
JAP	A533B	Steel B	63	1T-CT	TL	0.5	40
PRO	10KhMFTU		0–80	SE(B)	LS	0.5	30

6. TESTING AND EVALUATION PROCEDURES

The testing of the specimens and the evaluation of test results are based on ASTM Standard Test Method E 1921-02 [2]. The following technical recommendations were made:

- Side-grooving (SG) of 20% was recommended; note that not all laboratories used SG for the SE(B) tests while all of the 1T-CT tests utilized SG.
- Loading rate was requested to be reported and generally within a crosshead speed of 0.5 ± 0.1 mm/min; note that this range was not always used, but all laboratories used loading rates within the range allowed in ASTM E 1921-02.
- Unloading compliance techniques were recommended and used.

The J-integral at the onset of cleavage failure, J_c, of the test datum was determined following the recommendations in paragraph 9.1 of ASTM E 1921-02:

$$J_c = J_e + J_p \tag{6.1}$$

where,

J_e is the elastic component of the J-integral, and

J_p is the plastic component of the J-integral.

J_c values were transformed into plain strain cleavage fracture toughness values, K_{Jc}, using:

$$K_{Jc} = \sqrt{J_c \frac{E}{1-\nu^2}} \tag{6.2}$$

where,

E is the Young's modulus, and

ν is the Poisson's ratio for steel (0.3).

The measured K_{Jc} values were checked against the following defined validity criteria. A K_{Jc} datum was considered invalid if the specimen size requirement was exceeded:

$$K_{Jc(\lim it)} = \sqrt{\frac{E \cdot b_0 \cdot \sigma_{ys}}{M \cdot (1-\nu^2)}} \tag{6.3}$$

where,

b_0 is the initial cracked ligament (W-a_0),

M is the constraint value in ASTM E 1921-02 set equal to 30, and

σ_{ys} is the material yield strength at the test temperature.

For determining the reference temperature, T_0, the multi-temperature evaluation option of ASTM E 1921-02 was applied. T_0 was evaluated by an iterative solution to:

$$\sum_{i=1}^{n} \frac{\delta_i \cdot \exp\left[0{,}019 \cdot (T_i - T_0)\right]}{11 + 77 \cdot \exp\left[0{,}019 \cdot (T_i - T_0)\right]} - \sum_{i=1}^{n} \frac{(K_{JCi} - K_{\min})^4 \cdot \exp\left[0{,}019 \cdot (T_i - T_0)\right]}{\left(11 + 77 \cdot \exp\left(0{,}019 \cdot (T_i - T_0)\right)\right)^5} = 0 \tag{6.4}$$

where,

T_i is the test temperature corresponding to $K_{Jc(i)}$, and

δ_I is the censoring parameter: $\delta_i = 1$, if the $K_{Jc(i)}$ datum is valid (see Equation 6.3) or

$\delta_i = 0$, if the $K_{Jc(i)}$ datum is not valid and censored.

The Master Curve for median fracture probability was expressed by:

$$K_{Jc(mean)1T} = 30 + 70\exp\left[0{,}019(T - T_0)\right] \tag{6.5}$$

The upper and lower tolerance bounds were calculated using Equation (6.6) for the cumulative fracture probability levels of 1%, 5% and 95%:

$$K_{Jc(0.xx)} = 20 + \left[\ln\left(\frac{1}{1-0.xx}\right)\right]^{1/4} \left\{11 + 77\exp\left[0.019(T - T_0)\right]\right\} \tag{6.6}$$

where,

0.xx represents the cumulative probability level.

The test results for the individual laboratories were evaluated by each laboratory and re-evaluated using the Master Curve evaluation procedure from laboratory FZR. Before the re-

evaluation, the FZR procedure was validated against the Master Curve evaluation procedure of VTT (Finland Code FIN).

For the evaluation of the tests, the following conditions were specified:

- Young's modulus for the JRQ materials was assumed to be 207 GPa at 20°C and adopted to the test temperature according to:

$$E(T) = \frac{(1000 \cdot E(20°C) - (T - 20) \cdot 87)}{1000} \tag{6.7}$$

where,

E(T) is the Young's modulus at test temperature, T, and
E(20°C) is the Young's modulus at 20°C, assumed to be 207 GPa.

- The size adjustment is to 1T (25.4 mm) as specified in ASTM E 1921-02.
- K_{Jc} values lower than 50 $MPam^{0.5}$ need not size adjusted.
- Data censoring of K_{Jc} values > $K_{Jc(limit)}$ (see Equation 6.3) used σ_{ys} for the JRQ material as defined as a function of temperature using::

$$\sigma_{ys}(T) = 4 \cdot 10^{-8} \cdot T^4 - 2^{-5} \cdot T^3 + 3.6 \cdot 10^{-3} \cdot T^2 - 0.543 \cdot T + 490 \tag{6.8}$$

where

σ_{ys} (T) is the yield strength at the test temperature, T, in MPa. Note that other estimation formulas are available, but they generally produce the same results as Equation 6.8, especially at low temperatures where most testing has been conducted.

The Structural Integrity Assessment Procedures for European Industry (SINTAP) contain a Master Curve (MC) extension for statistically analyzing the fracture behavior of inhomogeneous ferritic steels with the aim to produce conservative reference temperatures. The SINTAP-MC procedure consists of three steps, and guides the user towards the most appropriate estimate of the reference temperature, T_0^{SINTAP}, of the investigated steels [15, 16]. The procedure is briefly described next.

Step 1: Standard Estimation

The measured K_{Jc} values are evaluated to determine the value of T_0 according to ASTM E 1921-02.

Step 2: Lower-Tail Estimation

K_{Jc} values of a data set above the fracture toughness curve for 50% failure probability, $K_{Jc(med)}$, are censored at the $K_{Jc(med)}$ value at the test temperature for the specific specimen. This process ensures that the estimate describes the material (i.e. microscopic properties), without being affected by macroscopic inhomogeneity, ductile tearing or large-scale yielding. Step 2 proceeds as a continuous iteration process until a "constant" level has been reached for T_0, which is termed T_0^{SINTAP}.

Step 3: Minimum Value Estimation

Only the minimum toughness value (i.e. one value corresponding to one single temperature) in the data set is used for the estimation. The intent is to assess the significance of a single minimum test result to avoid non-conservative fracture toughness estimates that may arise if $K_{Jc(med)}$ is used to express significant macroscopic inhomogeneity in a material. Step 3 leads to a conservative reference temperature, and it is intended for test series with less than 10 specimens. Step 3 was not applied in the re-evaluation presented here.

7. MASTER CURVE ANALYSIS OF JRQ MATERIAL

7.1. MASTER CURVE T_0 EVALUATIONS FOR THE DIFFERENT LABORATORIES

Tables 7.1 and 7.2 summarize the results of the re-evaluation for the Charpy size SE(B) specimens of the ¼-T and ¾-T locations and the ½-T location, respectively. The T_0 results are based on ASTM E 1921-02 for standard Master Curve predictions, the SINTAP-MC reference temperature, T_0^{SINTAP}, and the difference between these two values. When this difference gets to be large, there is a strong indication that the data set shows excessive scatter which may be indicative of material inhomogeneity or potentially some testing biases in cases where more than one laboratory has performed tests. The re-evaluated values of T_0 are compared with those determined and reported by each individual laboratory.

The differences between these T_0 values may result from several sources or evaluation assumptions. Small differences can result from the lack of a full evaluation by some laboratories as compared to the re-evaluation procedure used here; note that some data were recalculated by adjusting the J_{el} values by 1.3 N/mm to make all calculations follow a plane strain calculation. The application of the SINTAP MC approach leads to slightly higher reference temperatures compared with the standard ASTM E 1921-02 MC prediction for most of the test series.

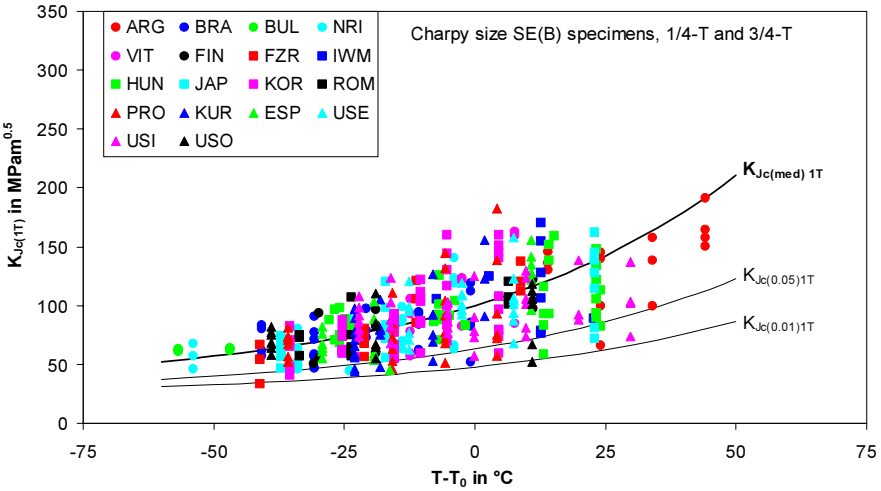

FIG. 7.1 – K_{Jc} Values Adjusted to 1T Specimen Size and Master Curve for Charpy Size SE(B) Specimens from the ¼-T and ¾-T Locations of Blocks of JRQ Tested by Different Laboratories (see Table 7.1).

Figures 7.1 and 7.2 show the K_{Jc} values versus test temperature normalized to the individual T_0 of the different laboratories. The K_{Jc} values adjusted to a specimen thickness of 1T follow the expected trend for the Master Curve (see the median curves, $K_{Jc(med)1T}$). Only a couple of K_{Jc} values are below the confidence level of 1% fracture probability ($K_{Jc(0.01)1T}$), which is near expectation of 3–4 from a data set of over 300 results. There may be a few more than expected data that fall near or below the 5% fracture probability lower bound ($K_{Jc(0.05)1T}$) indicating a slight amount of additional data scatter.

Table 7.1 – Evaluated T_0 and T_0^{SINTAP} for Charpy Size SE(B) Specimens from the ¼-T and ¾-T Locations for the Different Laboratories

Code	JRQ Block	Thickness Location (mm)	Re-Evaluation				Reported	Additional Information
			Σn_i	T_0 °C	T_0^{SINTAP} °C	$T_0 - T_0^{SINTAP}$ K	T_0 °C	
ARG	3JRQ	55	0.5	-94	-67	-27	-89	0% SG
BRA	6JRQ31	45	3.43	-59	-54	-5	-57	0% SG
BUL	5JRQ54	65	1.83	-53	-53	0	-49	J_{el}:. -1.3 N/mm, SG
NRI	6JRQ23	55	2.98	-56	-52	-4	-55	10% SG
VIT	6JRQ14	55	2.36	-58	-57	-1	-54	J_{el}:-1.3 N/mm, 0% SG
FIN	6JRQ21	55	1.19	-71	-62	-9	-67	20% SG
FZR	6JRQ12	55	1.9	-69	-66	-3	-69	20% SG
IWM	6JRQ43	55	0.83	-63	-53	-10	-58	0% SG
HUN	6JRQ33	55	4.41	-83	-77	-6	-77	20% SG
JAP	6JRQ51	61	2.11	-73	-63	-10	-71	20% SG
KOR	5JRQ25	55	6.9	-65	-63	-2	-64	0% SG
ROM	6JRQ22	55	1.62	-66	-63	-3	-61	20% SG
PRO	6JRQ44	55	3.81	-74	-64	-10	-69	0% SG
KUR	5JRQ33	55	3.43	-62	-57	-5	no	J_{el}:-1.3 N/mm, 20% SG
ESP	6JRQ34	55	1.88	-71	-67	-4	-70	0% SG
USE	5JRQ45	55	3.17	-77	-77	0	-72	0% SG
USI	5JRQ45	55	5.05	-100	-93	-7	-107 to -85*	J_{el}:-1.3 N/mm, 0% SG
USO	6JRQ13	55	2.44	-71	-68	-3	-70	20% SG

* Loading rates in the range of 0.5 to 0.01 mm/min were evaluated to test for a loading rate effect; also two different test laboratories were involved. A loading rate effect appears to exist within the range of allowable ASTM E 1921-02 rates; i.e., lower loading rates produce lower values of T_0. However, all of the data were combined in the re-evaluation procedure which resulted in a lower value of T_0 than for other participants.

The quantity identified in Table 7.1 as Σn_i is a summation for the individual set of data that identifies whether the dataset has enough non-censored test results to generate a valid measure of T_0 following ASTM E 1921-02. A value of Σn_i less than unity signifies an invalid data set. Two of the data sets identified in Table 7.1 are therefore invalid (ARG and IWM).

Table 7.2 – Evaluated T_0 and T_0^{SINTAP} for Charpy Size SE(B) Specimens from the ½-T Location for the Different Laboratories

Code	JRQ Block	Thickness Location (mm)	Re-Evaluation				Reported	Additional Information
			Σn_i	T_0 °C	T_0^{SINTAP} °C	$T_0 - T_0^{SINTAP}$ K	T_0 °C	
FIN	6JRQ21	112	1.02	-73	-68	-5	-68	20% SG
FZR	6JRQ12	112	1.43	-62	-62	0	-62	20% SG
USO	6JRQ13	119	0.86	-73	-70	-3	-72	20% SG

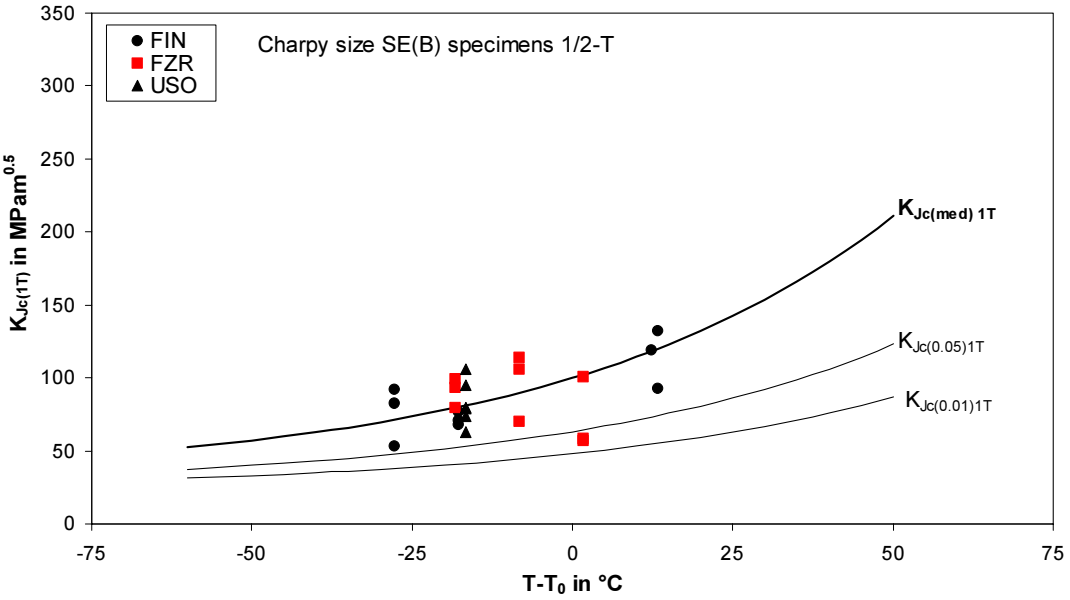

FIG. 7.2 – K_{Jc} Values Adjusted to 1T Specimen Size and Master Curve for Charpy Size SE(B) Specimens from the ½-T Location of the 6JRQ Plate Tested by Different Laboratories (see Table 7.2).

Tables 7.3 and 7.4 summarize the results of the re-evaluation for the 1T-CT specimens at the ¼-T and ¾-T locations and the ½-T location, respectively. Figures 7.3 and 7.4 show the K_{Jc} values versus the test temperature normalized to T_0 of the different laboratories. The K_{Jc} values also generally follow the course of the MC, though the scatter is large. Nevertheless, the K_{Jc} values are above the 1% fracture probability line.

Table 7.3 – Evaluated T_0 and T_0^{SINTAP} for 1T-CT Specimens from the ¼-T and ¾-T Locations for the Different Laboratories

Code	JRQ Block	Thickness Location (mm)	Re-Evaluation				Reported	Additional Information
			Σn_i	T_0 °C	T_0^{SINTAP} °C	$T_0 - T_0^{SINTAP}$ K	T_0 °C	
NRI	6JRQ23	55	0.75	-28	-11	-17	-33	0% SG
VIT	6JRQ14	66	1.45	-32	-24	-8	-39	J_{el} -1.3 N/mm, 0% SG
FZR	6JRQ12	55	1.93	-57	-54	-3	-57	20% SG
IWM	6JRQ43	55	2.18	-38	-38	0	-36	J_{el} -1.3 mm, 0% SG
ROM	6JRQ22	55	2.00	-63	-63	0	-60	20% SG
PRO	6JRQ44	55	1.33	-65	-65	0	-64	J_{el} –1.3 N/mm, 20% SG
USO	6JRQ13	55	1.75	-48	-41	-7	-48	J_{el} -1.3 N/mm, 20% SG

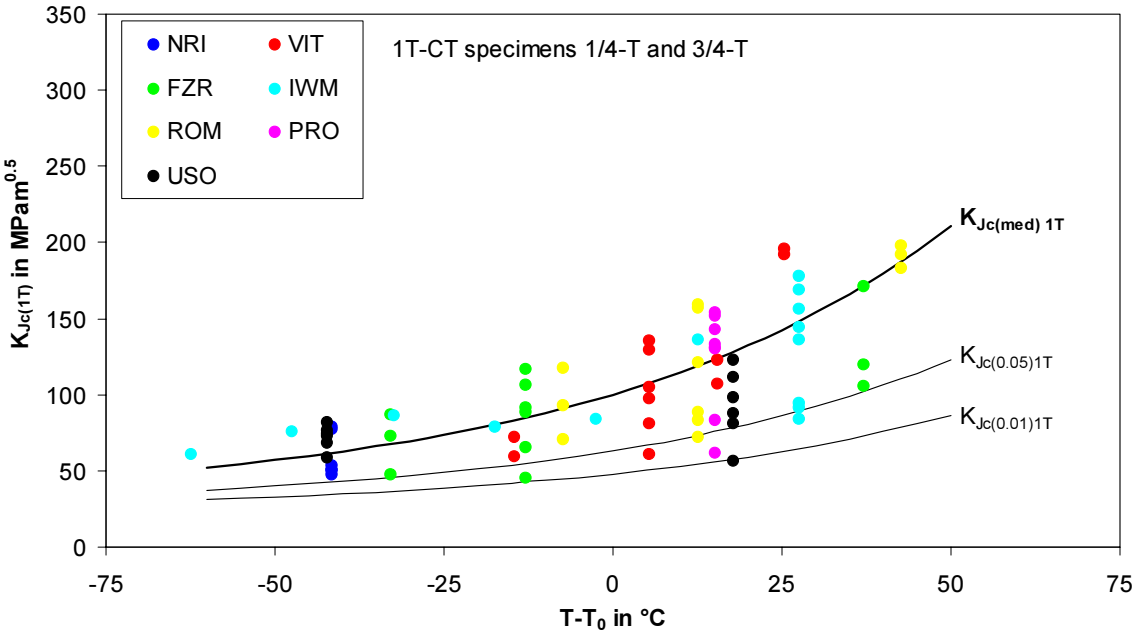

Figure 7.3 – K_{Jc} Values and Master Curve for 1T-CT Specimens from the ¼-T and ¾-T Locations of the 6JRQ Plate Tested by Different Laboratories (see Table 7.3).

Table 7.4 – Evaluated T_0 and T_0^{SINTAP} for 1T-CT Specimens from the ½-T Location for the Different Laboratories

Code	JRQ Block	Thickness Location (mm)	Re-Evaluation				Reported	Additional Information
			Σn_i	T_0 °C	T_0^{SINTAP} °C	$T_0 - T_0^{SINTAP}$ K	T_0 °C	
FZR	6JRQ12	112.0	1.00	-39	-33	-6	-39	20% SG
NRI	6JRQ23	112.5	1.13	-33	-33	0	-38	0% SG
USO	6JRQ13	119,0	1.5	-38	-18	-20	-38	J_{el} -1.3 N/mm, 20% SG

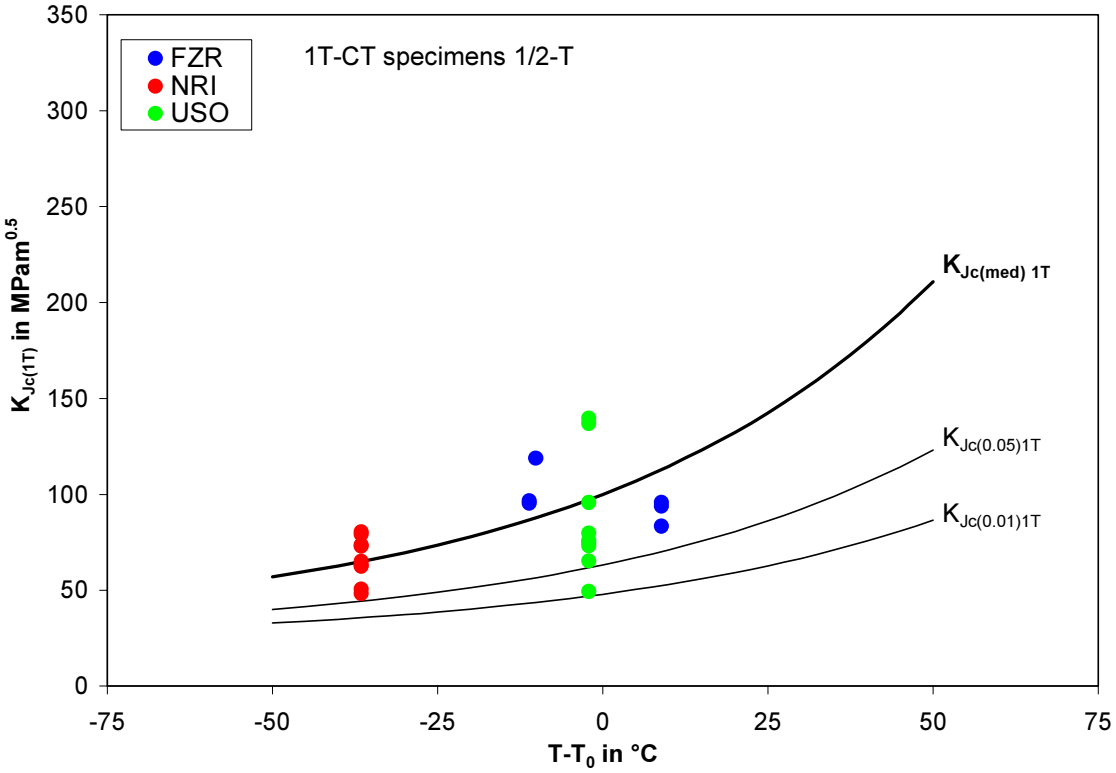

FIG. 7.4 – K_{Jc} Values and Master Curve for 1T-CT Specimens from the ½-T Location of the 6JRQ Plate Tested by Different Laboratories (see Table 7.4).

7.2. INVESTIGATION OF THE INFLUENCE OF TEST TEMPERATURE ON T_0

Tables 7.5 and 7.6 summarize only the 6JRQ plate test results re-evaluated for the Charpy size SE(B) and 1T-CT specimens tested at different temperatures for the ¼-T and ¾-T locations. Potential material variability between the JRQ plates was thus eliminated by only re-evaluating one specific plate which has a large amount of data. Figures 7.5 and 7.6 show the K_{Jc} values from the Charpy size SE(B) specimens versus the test temperature normalized to T_0 grouped for different test temperatures. Note that some specimens were tested at temperatures different than those identified in Table 7.5 and were therefore grouped with the closest test temperature. Figure 7.5 shows the K_{Jc} values versus test temperature normalized to

the individual T_0 at each test temperature. The overall Master Curve evaluation is shown in Figure 7.6, which illustrates the very small impact of using either the overall T_0 or T_0^{SINTAP}. Figure 7.7 plots T_0 values determined for each test temperature and the overall T_0 value for all of the combined Charpy size SE(B) data. The error band identified for each T_0 value is the uncertainty value as defined in ASTM E 1921-02 which is a function of the number of specimens tested. Except for the very lowest test temperature, the different T_0 values are very consistent. Caution when testing near the lowest test temperature allowed by ASTM E 1921-02 ($T_0 - 50^oC$) is warranted based on this data.

Similarly, Figures 7.8 and 7.9 show the K_{Jc} values from the 1T-CT specimens versus the test temperature normalized to T_0 and grouped for different test temperatures. The T_0 value determined for each test temperature was used in Figure 7.8, while the overall Master Curve evaluation is shown in Figure 7.9, which also illustrates the impact of using T_0 or the more conservative T_0^{SINTAP}. Figure 7.10 plots the T_0 values determined for each test temperature and the overall T_0 value for all of the 1T-CT data. As for the SE(B) data in Figure 7.7, the error band identified for each T_0 value is the uncertainty value as defined in ASTM E 1921-02. According to ASTM E 1921-02, the uncertainty of T_0 is defined as a standard two-tail normal deviation with the two variables, the test temperature and the number of specimens used for the T_0 determination, as:

$$\Delta T_0 = \frac{\beta}{\sqrt{r}} \cdot Z \qquad (7.1)$$

where

β = 18 - 20°C, depending on the value of $T-T_0$ (for single temperature data),
r is the number of valid (uncensored) test results used to determine T_0, and
Z is the confidence level ($Z_{85\%} = 1.44$).

When $K_{Jc(med)}$ is equal to or greater than 83 MPa√m, $\beta = 18^oC$. Alternatively, a value of $\beta = 20$ can be used for all values of $K_{Jc(med)}$ not less than the minimum of 58 MPa√m. The exact value of β can be determined from $K_{Jc(med)}$ according to ASTM E 1921-02.

Table 7.5 – Evaluated T_0 and T_0^{SINTAP} Dependence on Test Temperature for Charpy Size SE(B) Specimens from the ¼-T and ¾-T Locations in the 6JRQ Plate

Test Temperature °C	**Re-Evaluation**					**Laboratories**
	Σn_i	T_0 °C	ΔT_0 K	T_0^{SINTAP} °C	$T_0-T_0^{SINTAP}$ K	
-110	4.71	-79	4.7	-78	1	FZR, HUN, JAP, NRI, PRO, USO
-100	2.29	-68	6.8	-65	3	BRA, ESP, FIN, ROM
-90	8.71	-70	3.4	-61	9	BRA, ESP, FIN, FZR, HUN, JAP, NRI, PRO, ROM, USO
-80	3.67	-71	5.3	-63	8	BRA, FZR, PRO, NRI, VIT
-70	4.33	-64	4.7	-59	5	BRA, HUN, IWM, NRI, PRO, VIT
-60	4.17	-69	4.0	-68	1	BRA, ESP, FIN, FZR, HUN, NRI, ROM, USO
-50	1.17	-64	6.3	-52	12	IWM, JAP, VIT
All Values	10.95	-66	1.8	-61	5	

Table 7.6 – Evaluated T_0 and T_0^{SINTAP} Dependence on Test Temperature for 1T-CT Specimens from the ¼-T and ¾-T Locations in the 6JRQ Plate

Test Temperature °C	Re-Evaluation					Laboratories
	Σn_i	T_0 °C	ΔT_0 K	T_0^{SINTAP} °C	$T_0-T_0^{SINTAP}$ K	
-90	1.29	-60	9.0	-60	0	FZR, USO
-70	2.29	-55	6.5	-48	-7	FZR, IWM,NRI, ROM
-50	2.67	-63	6.5	-56	-7	ROM, PRO,VIT
-30	1.67	-27	8.2	-21	-6	USO, VIT
-20	1.50	-48	8.6	-46	-2	FZR, IWM, ROM, VIT
-10	1.50	-35	8.6	-35	0	VIT, IWM
All Values	10.74	-54	3.1	-41	-12	

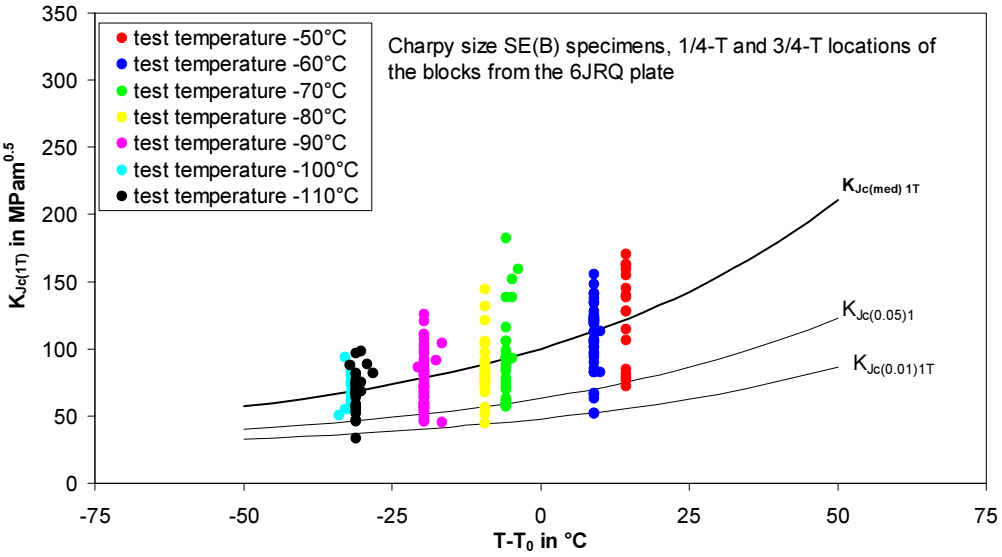

FIG. 7.5 – K_{Jc} Values Adjusted to 1T Specimen Size and Master Curve for Charpy Size SE(B) Specimens from the ¼-T and ¾-T Locations of the 6JRQ Plate Tested at Different Temperatures.

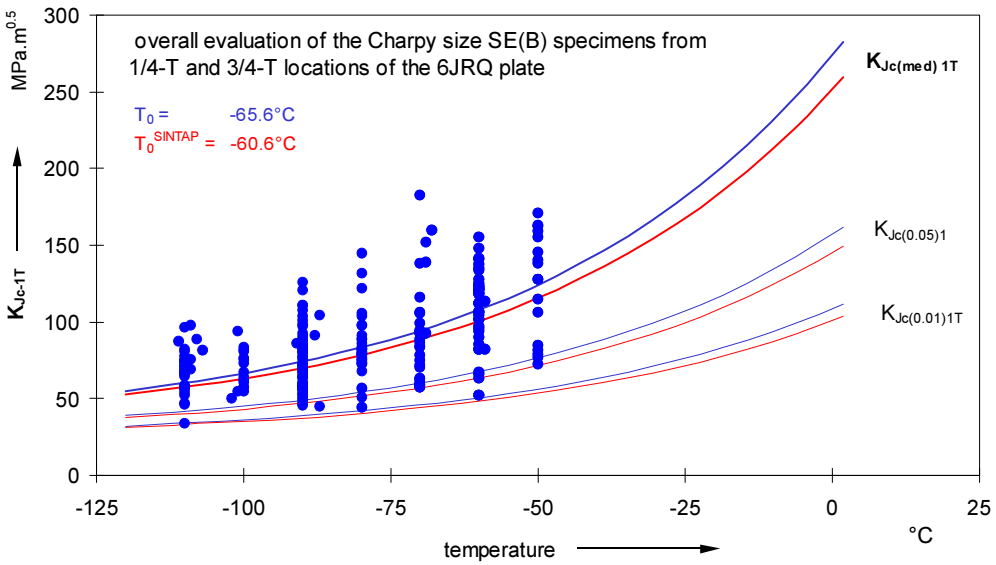

FIG. 7.6 – Overall Evaluation of K_{Jc} Values Adjusted to 1T Specimen Size and Master Curve for Charpy Size SE(B) Specimens from the ¼-T and ¾-T Locations of the 6JRQ Plate.

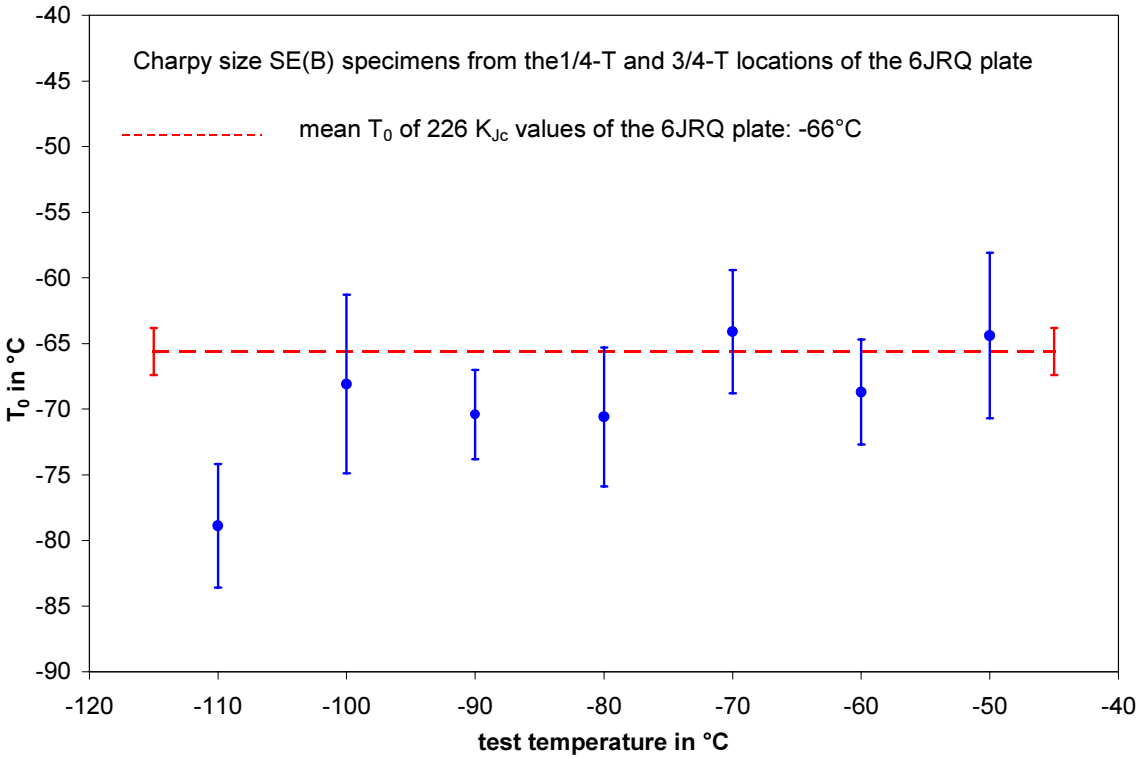

FIG. 7.7 – T_0 Dependence with Test Temperature for Charpy Size SE(B) Specimens from the ¼-T and ¾-T Locations of the 6JRQ Plate Tested at Different Temperatures.

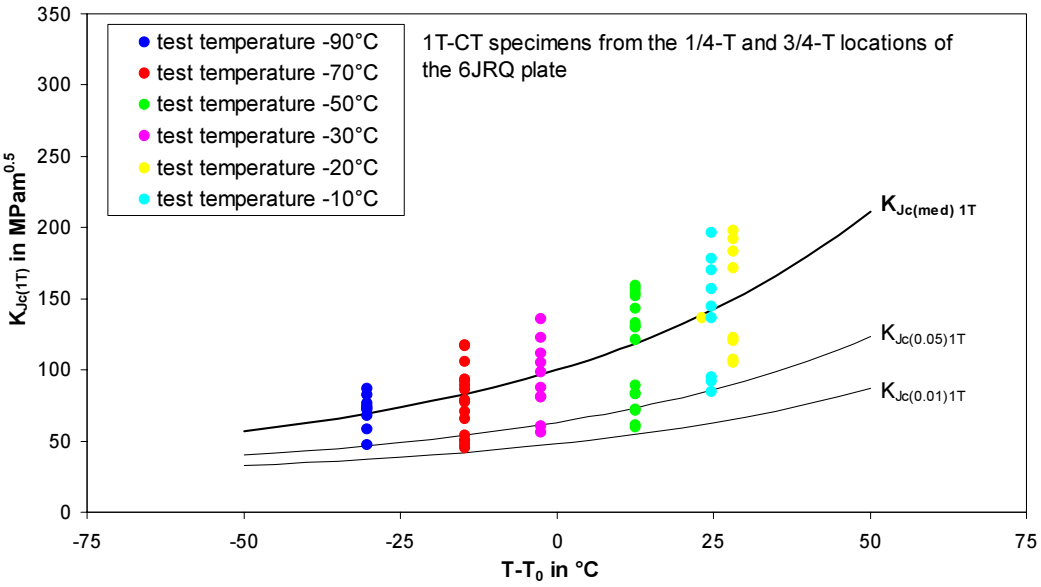

FIG. 7.8 – K_{Jc} Values and Master Curve for 1T-CT Specimens from the ¼-T and ¾-T Locations of the 6JRQ Plate Tested at Different Temperatures.

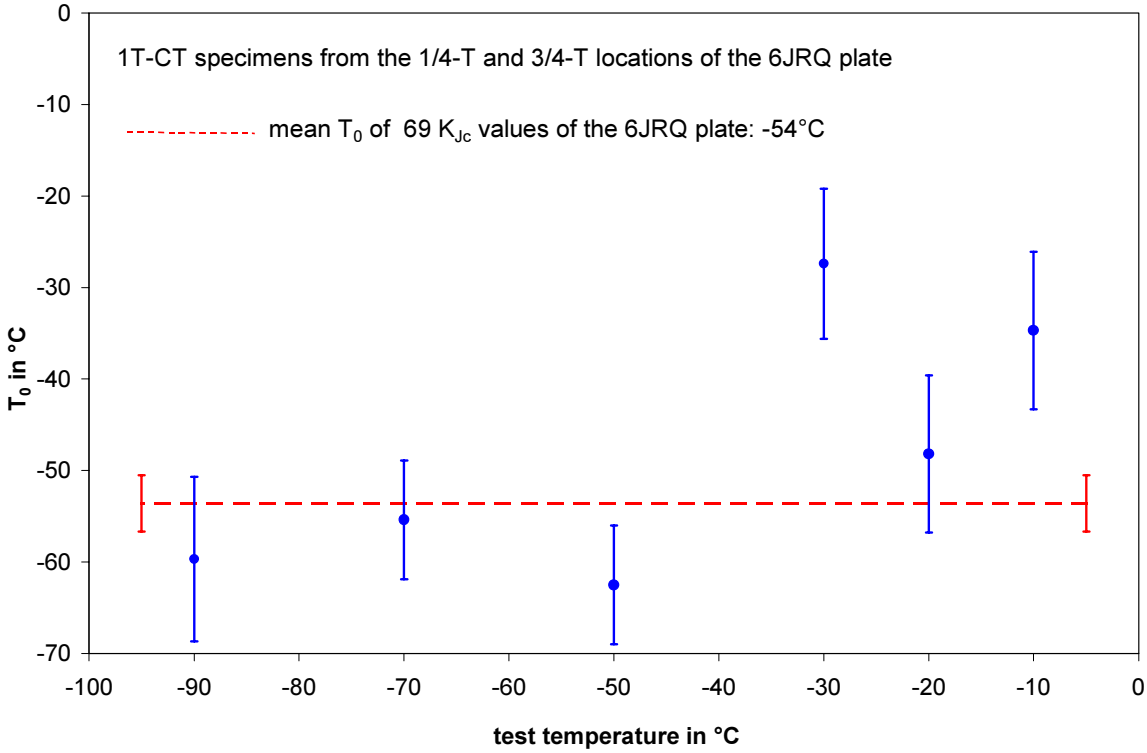

FIG. 7.9 – Overall Evaluation of K_{Jc} Values and Master Curve for 1T-CT Specimens from the ¼-T and ¾-T Locations of the 6JRQ Plate.

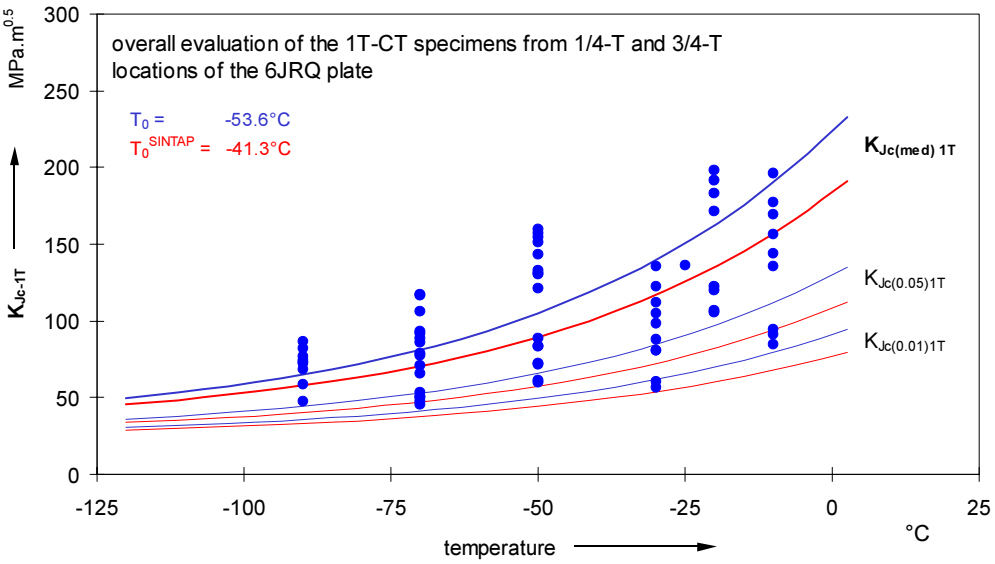

FIG. 7.10 – T_0 Dependence with Test Temperature for 1T-CT Specimens from the ¼-T and ¾-T Locations of the 6JRQ Plate Tested at Different Temperatures.

Except for the results at –30°C and –10°C, the T_0 values are very consistent. The reason for the deviation at these two temperatures is not known, but it is suspected that the reticularly arranged martensitic structure that has been identified in Figures 5.1 and 5.4 can lead to cases where local measurements of T_0 may be higher due to the localized higher hardness of the microstructure. Further metallographic work is needed to verify this assertion.

The difference between the overall T_0 values determined for the Charpy size SE(B) and 1T-CT specimens is 12°C for the 6JRQ plate. This value is consistent with other data that shows a difference between tests performed using Charpy size SE(B) and 1T-CT specimens. The difference between the overall T_0^{SINTAP} values determined for the Charpy size SE(B) and 1T-CT specimens is higher at 19°C for the 6JRQ plate. This larger difference is due to the 12°C higher value for the 1T-CT data; this larger deviation is a suggestion that material homogeneity may be an issue, such as the results at –30°C and 10°C.

8. MASTER CURVE ANALYSIS OF NATIONAL STEELS

The re-evaluation of the selected data identified in Table 5.7 is reflected in Figure 8.1 and Table 8.1. These national steels show a very consistent trend with the Master Curve. The national steels illustrate very little data scatter, and the two steels from JAP allow a check on the difference in measured T_0 between 1T-CT and Charpy size SE(B) specimens. The bias for JAP steel B is 6°C higher for the SE(B) tests, which is unusual but within typical data scatter. For JAP steel A, the bias is 2°C lower for the SE(B) tests which is more common. The difference in loading rates between the two tests also is different between the two test types, but consistent between the two materials. Therefore, this difference cannot be attributed to loading rate effects.

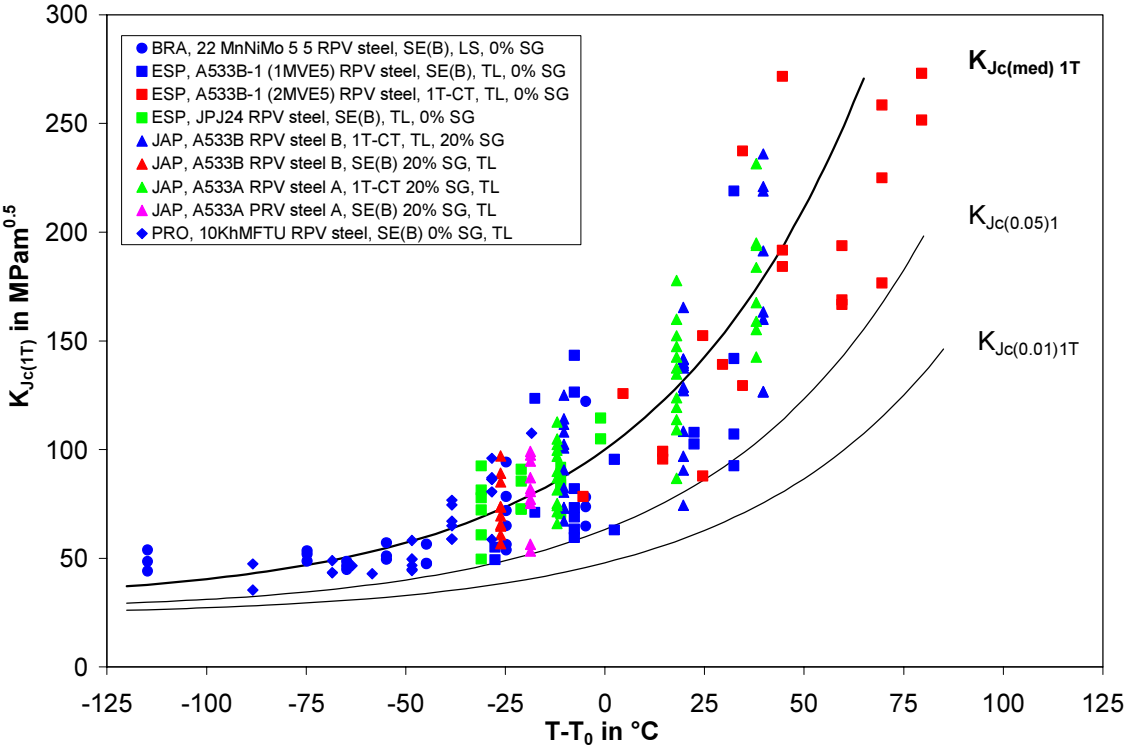

FIG. 8.1 – K_{Jc} Values Adjusted to 1T Specimen Size and Master Curve for the Evaluated National Materials.

Table 8.1 – Evaluated T_0 and T_0^{SINTAP} for National Materials

Type of Material	Material Code	Thickness Location (mm)	Specimen Type	Orientation	Loading Rate (mm/min)	Re-Evaluation				Reported
						Σn_i	T_0 °C	T_0^{SINTAP} °C	$T_0 - T_0^{SINTAP}$ K	T_0 °C
22 MnNiMo 5 5	--	--	SE(B)	LS	0.2	2.37	15	23	-8	17
A533B-1	1MVE5	43	SE(B)	TL	0.15	2.57	-132	-114	-18	-130
A533B-1	1MVE5	55	SE(B)	TL	300	2.1	-85	-71	-14	-83
A533B-1	2MVE51MVE.U1	43-74	1T-CT	TL	0.15	3.17	-115	-101	-14	-118
A533B-1	JPJ24	68	SE(B)	TL	0.15	2.6	-49	-49	0	-48
A533B	Steel A	67	SE(B)	TL	0.2	1.43	-71	-71	0	-71
A533B	Steel B	63	SE(B)	TL	0.2	1.43	-94	-94	0	-92
A533B	Steel A	63	1T-CT	TL	0.5	4	-69	-69	0	-66
A533B	Steel B	63	1T-CT	TL	0.5	6.38	-100	-100	0	-97
10KhMFTU	--	0-80	SE(B)	LS	0.5	2.98	-12	-10	-2	-18

9. NON-MANDATORY STUDIES – ADDITIONAL TESTS AND/OR EVALUATIONS ON JRQ STEEL AND NATIONAL MATERIALS

9.1. INTRODUCTION

As shown in Table 3.1 of Section 3, 13 of the 18 participants tested and/or evaluated one or more so-called “national steels.” This section presents a summary of those evaluations as they relate to the objectives of the CRP. Master Curve analyses of experimental data from these additional studies are reported in Section 8. The national materials were analysed to produce supplementary data for both conventional and abnormal materials/ material conditions to clarify the applicability of the Master Curve method in various situations. It is emphasised that inclusion of national materials was provisional and, therefore, these data alone do not form a complete database suitable for studying specific phenomena in a statistically reliable manner. These results should, therefore, be assessed mainly qualitatively to indicate trends of material behaviour that may be used to confirm the CRP observations and conclusions, or indicate areas that require additional investigations.

9.2. DISCUSSION OF NON-MANDATORY STUDIES

9.2.1. Summary of non-mandatory studies

Whereas the mandatory part of the CRP involved testing and analysis of the reference steel JRQ, the "national materials" of the programme are those tested in the non-mandatory part of the CRP. Table 9.1 provides a summary of the materials tested and any additional investigations performed in the non-mandatory portion, including the conduct of irradiation experiments. As shown in the table, most organizations tested one or several national materials or provided other supplementary test results. As stated previously, the data which were re-analysed using the Master Curve approach are discussed in Section 8 and will not be discussed here. The national materials consist variously of as-received, irradiated, annealed, reirradiated, thermally aged, and specially heat treated RPV base and weld metals of WWER-440, WWER-1000, and PWR materials.

For example, the mandatory WWER-1000 base and weld metals were tested by KUR both in the as-received and irradiated conditions, while HUN evaluated a WWER-440 weld in the irradiated (I), irradiated/annealed (IA), and re-irradiated (IAR) conditions. For PWR type materials, ESP, USE, USI, and USO tested materials in the post-irradiation condition. Regarding the use of thermal treatments, FIN performed a Master Curve analysis of an A387 RPV base metal which had been heat treated by ORNL to raise the transition temperature for the second Pressurized Thermal Shock Experiment (PTSE-2), while a thermally embrittled (low-temperature tempering) WWER 440 base metal and a corresponding weld metal manufactured using non-standard procedures were analysed by PRO.

Table 9.1 – Summary of National Steels and/or Additional Testing and Other Studies Performed

Country	Organization	Code	Tests of National Steel(s)			Other Evaluations
			Material Type	Kinds of Tests Performed	Irradiated Material	
Argentina	Comision Nacional de Energia Atomica	ARG	S.A. 508-2 and weld metal	K_{Jc} w/Charpy size SE(B) and 1TC(T)	No	No
Brazil	CNEN/CDTN	BRA	DIN 20 Mn Mo Ni 55	K_{Jc} w/Charpy size SE(B)	No	No
Bulgaria	Institute of Metal Science	BUL	No	N.A.	No	No
Czech Republic	Nuclear Research Institute	NRI	No	N.A.	No	No
Czech Republic	Vitkovice Research and Development.	VIT	WWER-440	K_{Jc} w/Charpy size SE(B)	No	JRQ Thru-thick, dK/dt both materials
Finland	VTT Industrial Systems	FIN	2¼Cr-1Mo	K_{Jc} w/Charpy size SE(B) and 1TC(T)	No	No
Germany	Forschungszentrum Rossendorf e.	FWM	No	N.A.	No	With JRQ: Dynamic K_{Jc} w/Charpy size SE(B), crack arrest K_a w/CVN impact
Germany	Fraunhoffer Institute fuer Werkstoffmechanik	FZR	No	N.A.	No	J-R tests w/JRQ and Metallographic studies
Hungary	Atomic Energy Research Institute	HUN	3 Welds (Irrad) and WWER-440 Weld 502 (I, IA, IAR)	K_{Jc} Master Curve	Yes	Yes
Japan	Japan Atomic Energy Research Institute	JAP	A533B-1 4 heats	KJc Master Curve w/Charpy size SE(B) and Dynamic impact K_{Jc} w/Charpy size	No	No

				SE(B)		
Korea, Republic of	Korea Atomic Energy Research Institute	KOR	A533B-Codes JFL and KFY5	Dynamic impact K_{Jc} w/Charpy size SE(B)	No	Subsize specimen tests w/JRQ.
Romania	Metallurgical Research Institute	ROM	Yes	No final report	No final report	No final report
Russian Federation	RRC "Kurchatov Institute"	KUR	WWER-440-ref and WWER-1000-ref + 2 fluences	K_{Jc} w/Charpy size SE(B)	Yes	No
Russian Federation	Prometey Institute	PRO	WWER-440-213 Base and Weld Metals	K_{Jc} w/SE(B) of 0.2T 0.4T, and 1TC(T)	No	15Cr2MoV in thermally embrittled condition
Spain	CIEMAT	ESP	A533B codes JPJ and MVE	K_{Jc} w/Charpy size SE(B) and 0.5TC(T) Dynamic K_{Jc} w/Charpy size SE(B)	Yes	SEM
United States of America	EPRI	USE	3 Welds, codes W5214, 34B009, and 27204	K_{Jc} w/Charpy size SE(B)	Yes	No
United States of America	ATI	USI	2 Welds, codes SA-1484 and WF-67	K_{Jc} w/Charpy size SE(B), 0.5TC(T), and 0.936T(RCT)	Yes	No
United States of America	Oak Ridge National Laboratory	USO	A533B HSST Plate 02 and HSSI Weld 72W	Charpy size SE(B), Sub-size Bend & C(T)	Yes	Subsize bend and subsize C(T) tests of JRQ and HSST Plate 02

Some additional studies were performed with the JRQ steel in the non-mandatory portion of the CRP. For example, VIT performed testing through the thickness of the plate and also performed high-rate loading fracture toughness tests of the JRQ steel and a WWER-440 national steel, while FWM conducted instrumented dynamic impact testing of Charpy size SE(B)[2] specimens to estimate a dynamic K_{Jc}, and instrumented impact testing of CVN specimens to estimate the crack-arrest toughness from the load-time signal. Additionally, FZR performed J-R tests of JRQ as well as extensive metallographic studies, while ESP reported the results of extensive scanning electron fractography. Subsize specimen tests of JRQ steel were conducted by USO and JAP, while USO also conducted subsize specimen testing of HSST Plate 02, and PRO conducted subsize bend tests of WWER-440 materials. Other dynamic tests with national steels, in the form of dynamic impact testing of Charpy size SE(B) specimens were performed by KOR, and ESP, while various loading rate tests were conducted by JAP with three national steels.

9.2.2. Results reported by participants

Only a brief summary of the results of these studies will be presented here. In some cases, a few plots of data will be included because they relate directly to the primary objectives of the CRP. In most cases, however, the most salient points, based on observations and conclusions contained in the presentations and reports from the participating organizations, are noted. In this regard, the observations and/or conclusions made by the participants are stated verbatim from their reports.

ARG, in an evaluation of single vs. multiple temperature analyses, concluded:

"Although the number of specimens tested maybe are not enough for a general conclusion, seems that the T_0 are lower for single temperature tests methodology, that is, are a little less conservative. Also the PCVN specimens are less conservative than the CT-1T specimens which is in agreement with other authors."

BRA performed both CVN and fracture toughness tests of JRQ steel and NUCLEP steel (20MnMoNi55) with the conclusion:

"The constants for test temperature selection based on Charpy results were not adequate for tests with IAEA and NUCLEP material. The temperatures T_0 are very different from T_{28J} –50ºC."

The values they reported are T_{28J} –23ºC and T_{28J} +59ºC for JRQ and NUCLEP, respectively.

VIT performed a substantial amount of testing of JRQ steel in various through-thickness locations and concluded:

"There is a significant effect of specimens location in the plate thickness of JRQ reference material. While T_0 in the depth equal to one quarter of the thickness is $T_0 = -50$ºC, T_0 in the depth equal to 4/4 t is $T_0 = -137$ºC." Thus, these experiments have demonstrated a decrease in T_0 of 87ºC from the quarter thickness to the surface of the plate. From their tests at different loading rates, VIT also concluded: "T_0 determined for both JRQ reference material and

[2] Fatigue precracked Charpy V-notch (CVN) size SE(B) specimens have a 10 mm square cross section and often referred to as PCVN specimens. This nomenclature is used in Table 9.1 and in this section.

WWER RPV material was found to be affected by loading rate within the allowable range of crosshead speeds."

Their report provides values for T_0 of –137ºC and –144ºC for loading rates of 0.5 mm/min and 0.05 mm/min, respectively.

FIN tested Charpy size SE(B) specimens of a Cr-Mo steel used for a Pressurized Thermal Shock cylinder test at ORNL as well as the CRP tests of JRQ steel and concluded:

"The results are consistent with the previous investigations, according to which there exists a small, probably 6–7ºC bias between the T_0 values measured with compact tension and those with (Charpy size) 3-point bend specimens. Because this temperature difference, which means that the fracture toughness estimate (T_0) measured with CT specimens is likely slightly more conservative than with 3-point bend specimens, is expected to be small, a bias correction for specimen type can so far be considered unnecessary."

FWM tested 1T-CT specimens of JRQ and observed T_0 values of –29 and –36ºC for the single and multiple temperature methods of analysis, respectively. Additionally, their impact testing of Charpy size SE(B) specimens resulted in a multiple temperature T_0 of –3ºC, showing a 33ºC increase in T_0 as the result of impact testing. Analysis of instrumented CVN impact tests showed an increasing crack-arrest load with increasing test temperature, which they fit with two different exponential equations. FWM did not provide written conclusions.

FZR, in addition to a large amount of testing and analyses of the JRQ steel, performed optical microscopy metallographic evaluations at the ¼, ½, and ¾-thickness locations and concluded:

"As it was expected the basic microstructure is bainitic. The bainite is preferentially lower bainite and martensite at the surface layer. In middle section the basic structure is heterogeneously composed upper bainite. Between ¼ and ¾ thickness (middle section) reticular arrangements of martensitic structure occur within the basic bainitic structure. The reticularly arranged martensitic structure becomes more pronounced in the thickness direction. The reticular arrangement must be explained by segregation. The hardness of the reticularly arranged martensitic structure is about 25% higher than the hardness of the matrix. The segregations were analysed by X ray spectroscopy (energy dispersive) and ion-beam. In summary, it can be said that the segregations show higher concentrations in the Cr (+15%), Mn (+23%), Cu (+20%), and Mo (+30%) contents compared with the matrix." A macrograph showing the segregation was shown earlier in Section 5, Figure 5.4.

HUN performed fracture toughness Master Curve analyses of four different welds in the unirradiated and irradiated conditions, including one of them in the annealed and reirradiated conditions (the well known WWER-440 Weld 502). No observations or conclusions were stated, but they showed plots of the data for three of the welds with fits of the Master Curve and curves for the 95% tolerance bound, the PNAE Code curve, and the Interatomenergo curve. In all three cases, the 95% tolerance bound provided a reasonable bounding curve to the data (about 10 specimens each for the unirradiated and irradiated conditions for each weld) with the PNAE and Interatomenergo curves slightly more conservative, respectively. For Weld 502, where the irradiation and reirradiation fluences were both 3×10^{23} n/m^2 (E>1 MeV), no data were shown but the Master Curve for the reirradiated case was at a somewhat higher temperature than that for the irradiated case.

JAP performed testing on four national steels, including high rate tests on three different heats of A533 grade B class 1 steel. They characterized the four steels as:

"Steel **A** similar to early 70s steel, modern-type low impurities steel (Steel **B** or **L**), and low toughness steel JSPS A533B."

For the loading rate tests, they used loading rates of 0.2 mm/min. (quasi-static), 10 mm/min., and 300 mm/min. They also performed K_{Jc} testing with Charpy size SE(B) and 1T-CT specimens of three steels and evaluated the results for Master Curve analysis by the single temperature and multi-temperature methods. Regarding the K_{Jc} testing, they concluded: "Multi-temperature analysis of PCCv data resulted in slightly lower T_0 value compared with T_0 values from single temp. method and 1T-CT results."

Regarding loading rate effects, they made the following observations: (1) T_0 increases as loading rate increases; and (2) T_0 shift tends to decrease as T_{0_static} increases. Further study is necessary. They showed a plot of their loading rate data compared with data of Yoon (JRQ) and Joyce (A515) and, although they did not offer a definitive statement about the comparison, the plot shows their data exhibited trends very similar to those of Joyce and Yoon.

KOR performed dynamic testing of JRQ steel and two national steels with Charpy size SE(B) specimens under impact loading. For the three steels tested under impact loading and referring to the fit of the Master Curve, they concluded:

"Compared with the slow bend test results, the slope seems to be too high."

KUR conducted Charpy size SE(B) testing of a WWER-440 base metal in the unirradiated condition, as well as a WWER-1000 weld metal in the unirradiated and at two different fluences in the irradiated condition. All evaluations of T_0 were performed with the single temperature method. In an evaluation of the Charpy size SE(B) estimate of T_0, they concluded:

"The substantial scatter of (T_{28J}-T_0) values is observed. It points to some uncertainty in the choice of fracture toughness testing temperature."

For those national steels results, they observed differences in (T_{28J}-T_0) from 14 to 70ºC.

PRO tested JRQ steel using two different specimen sizes, WWER-440 weld metal using three different specimen sizes, and a WWER-440 base metal in a specially heat treated condition using two different specimens sizes. The WWER-440 base metal thermal heat treatment was a low temperature tempering incorporated to increase the tensile strengths and increase the fracture toughness transition temperature as a means to somewhat model the material in the irradiated condition. Some of their observations are as follows:

1. For the JRQ steel, test results from Charpy size SE(B) specimens resulted in the following conclusions: "Mono- and multi-temperature calculations made on data for JRQ and SE(B)-0.4T specimens tested have resulted in T_0 = –72…–66ºC practically independently of test temperature in the range of –110…–70ºC. CT-1T experimental points are localized within the field limited by the tolerance bounds found for SE(B)-0.4T specimen Master Curve."

2. Regarding the WWER-440 weld metal tests (both Charpy size SE(B) and 5 × 10 mm cross-section), they concluded: "A reliable coincidence is observed between multi-temperature T_0 values determined by SE(B)-0.2T, SE(B)-0.4T, and CT-1T specimens tests of the steel weld of 15Cr2MoV metal though some tendency of T_0 elevation observed with specimen thickness increase. The increased slope parameter (values are observed for TPF (three parameter fitting)-curves of all three specimen types of this material." In this case, they did not report the results as a function of specimen thickness.
3. Regarding the base metal tests, they concluded: "Multi-temperature T_0 and T_Q values measured using two specimen types for thermally embrittled 15Cr2hMoV grade steel (σ_y = 730 MPa, T_{41J} = +75ºC) have shown a noticeable difference (~25ºC) between SE(B)-0.2T and CT specimens." The fracture toughness temperature dependence of this material is well described by three-parameter exponential function with the slope parameter . As result, a systematic trend of mono-temperature T_0 growth with the test temperature growing takes a place. Real lower shelf of $K_{Jc}(T)$ dependence of tested material is 10–20% lower as compared to this characteristic of Master Curve.

ESP performed a substantial amount of additional testing, including testing of JRQ in the irradiated condition and in two different orientations, testing of two national steels, dynamic testing of JRQ and one national steel, evaluation of specimen thickness, and detailed microstructural evaluations using SEM and AUGER analysis. Some of their observations are as follows:

1. "Results presented in this report for irradiated JRQ material show a difference of 25ºC between the T_0 value determined with PCVN ($T_{0(PCVN)}$ specimens and 1/2TCT ($T_{0(1/2TCT)}$) specimens, that is:

   $$\text{Irradiated JRQ: } T_{0(PCVN)} - T_{0(1/2TCT)} = -24\text{-}1 = -25ºC.$$

   This T_0 bias due to specimen geometry is higher than other biases published in the literature for non-irradiated data, which is around −10ºC. Anyhow, other authors reported as value up to −35ºC for T_0(PCVN) − T_0(1TCT)."

2. "CIEMAT T_0(PCVN) and T_0(1/2TCT) values for non-irradiated JRQ tests that gave a difference of −22ºC. For MVE material T_0(PCVN) and T_0(1TCT) gave a difference of −10ºC."

3. "In the case of MVE material, three specimens geometries were tested (PCVN, 1/2TCT and 1TCT). The less conservative T_0 value was determined testing PCVN specimens [T_0(PCVN) = −130ºC] and the most conservative one was determined testing 1/2TCT specimens [T_0(1/2TCT) = −85ºC]. 1TCT specimen testing gives an intermediate T_0value [T_0(1TCT) = −118ºC]."

4. "Comparing the results of this material for a testing rate of 0.15 mm/min with different orientation (TS and TL) no effect of specimen orientation can be deduced."

5. "The T_0 due to neutron irradiation for both fracture toughness specimens geometries is similar, but caution should be taken because the nonirradiated T_0 values are very different:

Non-Irradiated PCVN T_0 = –70ºC

Non-Irradiated 1/2TCT T_0 = –48ºC"

Thus, based on these results, ESP concluded:" if non-irradiated T_0 value is determined by testing PCVN specimens and irradiated T_0 value is determined by testing 1/2TCT specimens, a bias term of 25ºC should be added to non-irradiated T_0 value in order to reach the more conservative irradiated T_0 value."

6. Referring to their tests at dK/dt values of 5 MPa√m/s, 50 MPa√m/s, and 1000 MPa√m/s, and the relationship,

$$T_{0(estimated)} = T_{0(static)} + 5.33 \ln\{(dK/dt)/0.5\},$$

they observed: "For JRQ material, this lineal relationship works very well, while for MVE material some discrepancy can be seen." They further observed: "Anyway, some authors report a greater effect of loading rate when the static T_0 value is very low, that is the case of MVE material."

7. "Auger microchemical analysis of non-irradiated JRQ material was performed in the past by CIEMAT in order to study grain boundary segregation. This analysis revealed the presence of phosphorous in atomic concentrations close to 2%. That could be associated with the presence of IGF even for non-irradiated JRQ material." Regarding the JRQ specimens tested for this CRP, ESP observed: "A careful SEM examination was performed on all the specimens tested and also revealed the presence of small IGF areas for non-irradiated and irradiated specimens."

USE tested and evaluated irradiation effects on the reference temperature shift for three different RPV welds. Charpy size SE(B) specimens were tested in all cases and reconstituted specimens were used for all irradiated specimens. The neutron fluence for all three materials was 1.62×10^{19} n/cm^2 (E > 1 MeV). While they did not make any conclusions, they did report irradiation-induced shifts of 133, 148, and 179ºC.

USI tested two different power reactor RPV weld metals in the unirradiated and irradiated conditions using Charpy size SE(B), 0.5TC(T), and 0.936T-RCT specimens. At the time of preparation of this TECDOC, however, the data were not publically releasable.

USO performed testing of one RPV weld to compare Charpy size SE(B) and 1T-CT results, and also performed subsize specimen tests of JRQ and another RPV reference steel. The results shown below in Figure 9.1 (taken from the USO final report on the CRP) provide a comparison of test results from a Materials Properties Council (MPC) round robin project that used Charpy size SE(B) specimens with 1T-CT specimens tested by ORNL. More than 250 Charpy size SE(B) specimens of HSSI Weld 72W were tested in the round robin project and the dashed line in Figure 9.1 shows the Master Curve for those data. A total of 45 1T-CT specimens of HSSI Weld 72W were tested by ORNL and the solid curve shows the Master Curve for those data. From these results, USO concluded:

"Similar testing of a national material, HSSI Weld 72W, showed similar results, with PCVN specimens giving a T_0 value 21ºC lower than that for 1TC(T) specimens."

This result compares with a difference of 12ºC between Charpy size SE(B) and 1T-CT for the JRQ steel obtained from the Fifth CRP results in this TECDOC.

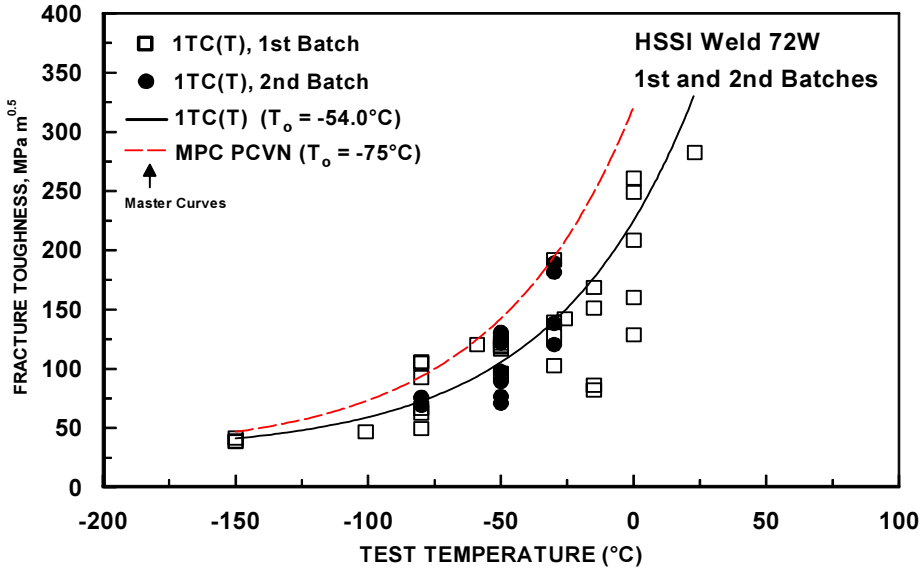

FIG. 9.1 – Fracture Toughness Results from ORNL Tests with 1T-CT Specimens of Unirradiated HSSI Weld 72W Compared with the Master Curve Based on Test Results from an MPC Round Robin Program with More Than 250 Charpy Size SE(B) Specimens.

Regarding testing of subsize specimens of two different A533 grade B class 1 plates, USO observed:

"Testing of subsize specimens from JRQ Plate and HSST Plate 02 showed that T_0 determined from PCVN specimens with W/B=1, on average, is lower than T_0 determined from compact specimens with W/B=2. Moreover, 5x10x55 mm three-point bend specimens with W/B=2 exhibited T_0 values that were very similar to T_0 values derived from compact specimens. However, these results indicate a need for further experimental and analytical work to resolve the reasons for these observations from both constraint and J-integral formulas points of view."

9.3. COMPARISON OF SUBSIZE SPECIMEN TESTS

As discussed above, some studies were performed by PRO and USO with subsize specimens of both bend and compact types. For example, Table 9.2 shows results from USO with all specimens tested at –100ºC. The T_0 values range from –67 to –76ºC, with the value of –76ºC resulting from the normal Charpy size SE(B) specimen. These results compare with the T_0 of –65ºC from the Charpy size SE(B) specimens obtained from the Fifth CRP results discussed in Section 8.

Table 9.2 – Comparisons of Fracture Toughness Data for Subsize Specimens with Charpy Size SE(B) and CT Specimens

Material	Test Temp(s), °C	Specimen Type	N/r[a]	$K_{Jc\ (med)}$, MPa-$m^{1/2}$	T_0 or T_Q, °C
USO Tests of A533B Plate JRQ	-100	Charpy size SE(B): 10x10x55mm	20/20	88.76	-76.4
		5x10x55mm SE(B)	6/6	98.76	-73.9
		5x5x27.5mm SE(B)	6/4	84.56	N/A
		0.4T-CT	8/8	79.37	-66.8
		0.2T-CT	7/7	97.66	-73.0
USO Tests of A533B HSST Plate 02	-30	10x10x55mm SE(B)	7/5	121.3	N/A
		5x10x55mm SE(B)	10/8	112.5	-14.2
	-50	10x10x55mm SE(B)	7/7	89.0	-26.6
		5x10x55mm SE(B)	8/8	75.7	-0.3
		5x5x27.5mm SE(B)	12/6	97.0	N/A
		0.4T-CT	6/6	75.8	-12.6
		0.2T-CT	6/6	74.5	1.3
PRO Tests of 15Cr2MoV Base Metal-Special H.T.	-25 to 20	0.2T-SE(B)		Multi-temp	20.6
	0 to 105	1T-CT		Multi-temp	44.7
PRO Tests of 15Cr2MoV Weld Metal	-60 to -30	0.2T-SE(B)		Multi-temp	-19.8
	-50 to -30	Charpy size SE(B)		Multi-temp	-17.5
	-40 to 20	1TC(T)		Multi-temp	-30

[a] N is number of specimens tested, r is number of valid tests by ASTM E1921-02.

A summary of the observations is as follows:

1. USO noted that SE(B) specimens with the same W/B ratio as standard compact specimens (W/B=2), give similar T_0 results, but that SE(B) specimens with W/B=1 tend to give lower T_0 values.
2. PRO noted that SE(B) specimens with W/B=1, but of two different thicknesses gave similar T_0 values as those from 1T-CT specimens for a weld metal, but noted a difference of 25ºC for similar size specimens of a base metal.

Thus, it is noted for this CRP that the results from testing of subsize bend and compact specimens provide mixed results and there is a strong need for further experimental and analytical evaluations.

9.4. OBSERVATIONS REGARDING T_0 DIFFERENCES BETWEEN BEND AND COMPACT SPECIMENS

As discussed previously, some of the organizations compared T_0 values for different types of specimens for their testing of national steels. A summary of the reported results is presented next. FIN tests with a specially heat treated RPV steel resulted in a T_0 of 6 to 7ºC lower for the Charpy size SE(B) specimens relative to that from CT specimens.

PRO tests with a WWER-440 base metal resulted in a difference of ~25ºC between SE(B)-0.2T and CT specimens, with the SE(B) specimen giving the lower value. ESP reported the following separate test results with different specimen types:

1. For irradiated JRQ material, the observed a difference of 25ºC between the T_0 value determined with 1/2T-CT specimens, with the Charpy size SE(B) specimen giving the lower value.
2. For non-irradiated JRQ tests with the same specimen types, the Charpy size SE(B) specimen gave a T_0 value 22ºC lower.
3. For the national steel MVE, three different specimen types were tested, Charpy size SE(B), 1/2T-CT, and 1T-CT). The T_0 value for the Charpy size SE(B) specimen was 45ºC and 12ºC lower than that for the 1/2T-CT and 1T-CT specimens, respectively.

USO reported a T_0 difference of 21ºC between Charpy size SE(B) and 1T-CT specimens for an RPV weld metal, with the Charpy size SE(B) specimens giving the lower value.

Thus, four organizations reported seven cases of T_0 comparisons with SE(B) and CT specimens, with the SE(B) specimen giving the lower T_0 in every case. The differences ranged from 12 to 45ºC, with an average value of 22ºC.

9.5. OBSERVATIONS REGARDING LOADING RATE EFFECTS

As mentioned previously, some of the organizations performed fracture toughness tests at different loading rates. The following is a summary of the various observations.

1. VIT conducted tests with two loading rates within the allowable range of crosshead speeds and observed T_0 values of –137ºC and –144ºC for loading rates of 0.5 mm/min and 0.05 mm/min, respectively.
2. JAP conducted tests at low and high loading rates and concluded that T_0 increases as loading rate increases, and the T_0 shift due to loading rate tends to decrease as T_{0_static} increases. Their loading rate data showed results similar to those of Yoon (JRQ) and Joyce (A515).
3. KOR performed dynamic tests under impact loading and compared the results with the shape of the Master Curve. They concluded that the slope of the curve fit seemed to be too high compared with that of the Master Curve.
4. ESP performed tests at dK/dt values of 5 MPa√m/s, 50 MPa√m/s, and 1000 MPa√m/s and they observed that a linear fit to the results works well. They also observed a greater effect of loading rate when the static T_0 value is very low.

10. COMPARISON OF RESULTS WITH PREVIOUS CRPs

One of the most important achievements from the Third Phase CRP,"Optimising Reactor Pressure Vessel Surveillance Programmes and their Analyses," was the acquisition of the IAEA reference steel JRQ. This steel was available for the Phase 4 and Phase 5 CRPs, as well as for irradiation and other studies in the IAEA member countries. JRQ was used as a common test material for CRP Phases 4 and 5 to test the Master Curve test method for use with small specimen, surveillance type material. While CRP Phases 1–3 were concentrated mostly on studies of irradiation effects, CRP Phases 4 and 5 switched to a study of key parameters for small specimen fracture mechanics. Due to the large number of test results obtained from Phases 3–5, a large database of fracture toughness and other results obtained on the JRQ steel is available for further analysis and comparison.

The fracture toughness measurements made in CRP Phase 3 must be viewed with some caution, however, since they were obtained before an official standard test method was available for Master Curve evaluation. CRP Phase 4 was conducted during the development of ASTM E 1921-97, and ASTM E 1921-02 was the method that evolved during the conduct of Phase 5. From this point of view, results from previous CRPs, mainly from CRP-3, must be analysed considering this historical development and the fact that each CRPs primarily used a different steel block taken from the JRQ plates [8]. The original ingot for JRQ was forged and rolled into two plates with dimensions of 2000 mm x 3000 mm x 225 mm and then were cut into test blocks with dimensions of 1000 mm x 1000 mm x 225 mm. One test block primarily was used for each CRP; plate A was cut into six sections as shown in Figure 10.1, and the sections have been used as follows:

- CRP Phase 3 – Section 3 JRQ
- CRP Phase 4 – Section 5 JRQ
- CRP Phase 5 – Section 6 JRQ

10.1. TENSILE PROPERTIES FOR JRQ

The tensile properties for the JRQ material are important due to their use in the censoring process in the determination of the T_0 temperature when following ASTM E 1921. The tensile yield strength (σ_{ys}) is the key parameter, and values were obtained in CRP Phase 4 with the following temperature dependence determined following the form used by the Welding Institute:

$$\sigma_{ys}(T) = 490 + 55555 / (T + 273) - 189 \qquad (10.1)$$

where σ_{ys} (T) is the yield strength (MPa) at the test temperature, T (^{o}C). The form of this relationship can also be expressed in a polynomial form [7] as was specified earlier using Equation (6.8):

$$\sigma_{ys}(T) = 4 \cdot 10^{-8} \cdot T^4 - 2^{-5} \cdot T^3 + 3.6 \cdot 10^{-3} \cdot T^2 - 0.543 \cdot T + 490 \qquad (6.8)$$

PLATE A

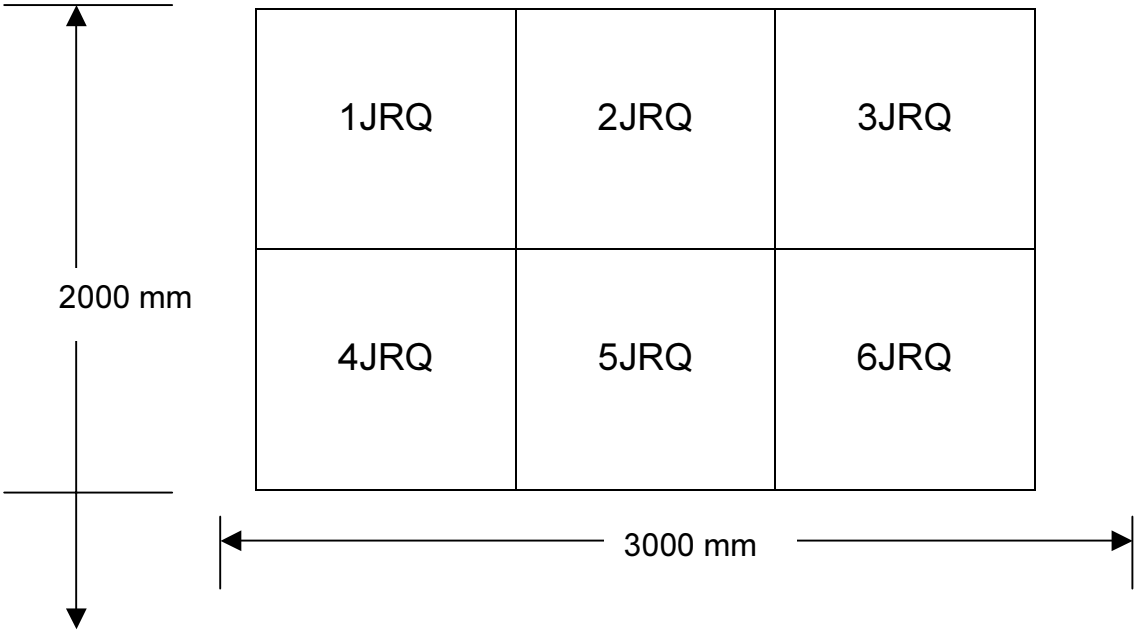

FIG. 10.1 – Cutting of Plate A into Test Sections with Dimensions 1000 mm × 1000 mm.

Figure 10.2 shows a comparison of experimental data of yield strength from the Fifth CRP at a location equal to 55 mm from the plate surface (1/4-T). It is clearly seen that there is practically no difference between these two approximations, and both nicely fit all experimental data.

10.2. CHARPY IMPACT TRANSITION TEMPERATURES

Charpy V-notch impact testing is the most commonly used method for characterizing the toughness of ferritic RPV steels. This inexpensive test can be used for assessing material quality and homogeneity, as well.

Table 10.1 shows a comparison of transition temperatures T_{41J} determined during the Third, Fourth, and Fifth CRPs for specimens located in depth equal to 55 mm (1/4-T).

Table 10.1 – Comparison of Charpy V-notch Impact Transition Temperatures for the JRQ plate in the T-L Orientation, 55 mm Depth

Charpy V-notch Tests	**CRP-3 (3JRQ)**	**CRP-4 (5JRQ)**	**CRP-5 (6JRQ)**
T_{41J}	$-15.9 \pm 8.2^{o}C$	$-23.6 \pm 5.7^{o}C$	$-20.0 \pm 11.4^{o}C$

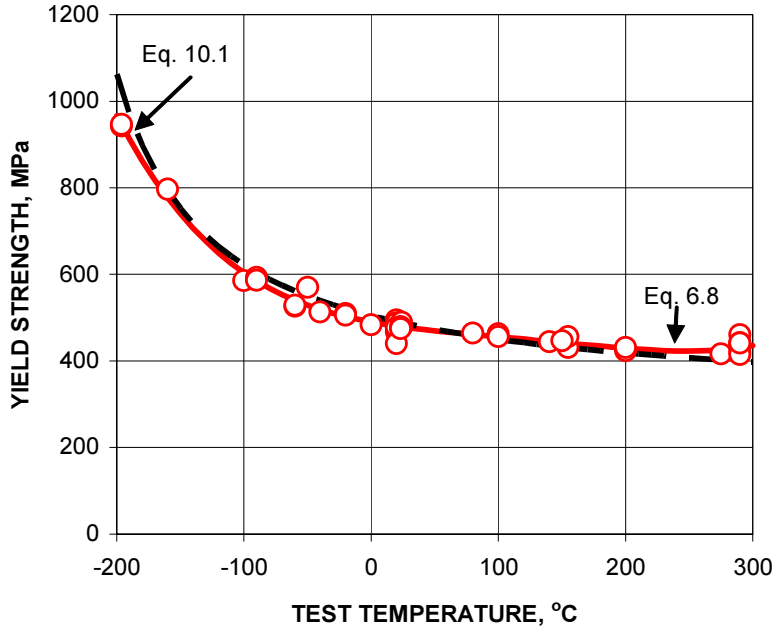

FIG. 10.2 – Comparison of Yield Strength Temperature Dependencies in JRQ Material.

These T_{41J} results represent mean values for an entire test section of 1000 mm x 1000 mm. From 20 to 30 individual blocks of each test section were used by the different laboratories involved. Figure 10.3 illustrates the similar transition temperatures, T_{28J}, measured for individual sections of test section 5JRQ. Also indicated in Figure 10.3 are the measured T_0 values (discussed next) obtained from the Fourth and Fifth CRPs. The variation in values provides insight into the homogeneity of the material within the area of 1 m^2. The scatter in the data is not abnormal and is typical for RPV steels.

10.3. STATIC FRACTURE TOUGHNESS RESULTS

Static fracture toughness testing on the JRQ plate was conducted as mentioned earlier starting with the Third CRP. The results from the Third CRP should be viewed cautiously as discussed earlier. Nevertheless, Table 10.2 provides a relative comparison of results as obtained in all CRPs. The T_0 results from the Fourth and Fifth CRPs on section 5JRQ are indicated in Figure 10.3. Note that some of the countries and laboratories did not participate in all three CRPs; for those not involved in the Fifth CRP, the country/laboratory coding is identified in Figure 10.3.

Table 10.2 shows the excellent agreement between results from Phases 4 and 5 even when different test sections (5JRQ and 6JRQ) were tested. This indicates that JRQ generally is macroscopically homogenous and test methods are comparable between individual laboratories. Somewhat lower values of reference temperature T_0 were obtained within the Third CRP. Note that only a few laboratories performed static fracture toughness tests in Phase 3 and their testing conditions did not fulfill all ASTM E 1921 validity requirements.

However, the results from Charpy impact tests, as listed in Table 10.1 show somewhat lower values of T_{41J} for the 5JRQ and 6JRQ sections as compared to the 3JRQ section, which is consistent with an expected higher value of T_0 for the 3JRQ section. The results are reasonably consistent within each test section except when invalid results may exist.

5JRQ11 ARG T_{28J} = -22°C **T_0 = -68°C**	***5JRQ12*** Belgium (BEL) T_{28J} = -17°C **T_0 = -63°C**	***5JRQ13*** BRA T_{28J} = -16°C **T_0 = -71°C**	***5JRQ14*** VIT T_{28J} = -22°C **T_0 = -73°C**	***5JRQ15*** NRI T_{28J} = -15°C **T_0 = -80°C**	***5JRQ16*** FIN T_{28J} = -22°C **T_0 = -66°C**
5JRQ21 Germany (MPA) **T_0 = -87°C**	***5JRQ22*** FZR T_{28J} = -22/-20°C **T_0 = -70/-64°C**	***5JRQ23*** HUN T_{28J} = -41°C **T_0 = -63°C**	***5JRQ24*** India (IND) T_{28J} = -34°C **T_0 = -78°C**	***5JRQ25*** KOR **T_0 = -65°C** **(CRP-5)**	***5JRQ26*** KOR T_{28J} = -15°C **T_0 = -67°C**
5JRQ31 Netherlands (ECN) T_{28J} = -30°C **T_0 = -53°C**	***5JRQ32*** ROM T_{28J} = -22°C **T_0 = -69/-72°C**	***5JRQ33*** KUR T_{28J} = -28°C **T_0 = -81°C/ -62°C (CRP-5)**	***5JRQ34***	***5JRQ35*** ESP T_{28J} = -18°C **T_0 = -70°C**	***5JRQ36***
5JRQ41 USO T_{28J} = -35/-32°C **T_0 = -77/67°C**	***5JRQ42*** Austria (AUS) T_{28J} = -17°C **T_0 = -71°C**	***5JRQ43*** JAP T_{28J} = -25°C **T_0 = -50°C**	***5JRQ44*** France (CEN) T_{28J} = -23°C **T_0 = -80°C**	***5JRQ45*** USE/USI T_{28J} = -30°C **T_0 = -76°C/ -77°C (CRP-5)**	***5JRQ46***
5JRQ51	***5JRQ52*** FWM T_{28J} = -33°C **T_0 = -76°C**	***5JRQ53***	***5JRQ54*** BUL **T_0 = -53°C** **(CRP-5)**	***5JRQ55***	***5JRQ56***

FIG. 10.3 – Distribution of Test Blocks for Laboratories and Results of Tests for Section 5JRQ (1 m × 1 m size).

Table 10.2 – Comparison of T_0 Results for SE(B) Specimens from Different Laboratories in CRP Phases 3, 4, and 5

Lab Code	CRP Phase 5/T-L			CRP Phase 4/T-L			CRP Phase 3/T-L			CRP Phase 3/L-T		
	Block	Depth mm	T_0 °C	Block	Depth mm	T_0 °C	Block	Depth mm	T_0 °C	Block	Depth mm	T_0 °C
ARG	3JRQ11	55	-94	5JRQ11	65	- 68				3JRQ11	100	- 53
BEL				5JRQ12	56	- 63						
BRA	6JRQ31	45	-59	5JRQ13	45	- 71						
BUL	5JRQ54	65	-53									
NRI	6JRQ23	55	-56	5JRQ15	55	- 80	3JRQ61	52	- 55			
VIT	6JRQ14	55	-58	5JRQ14	56	- 73						
FIN	6JRQ21	55	-71	5JRQ16	75	- 66				3JRQ	55	-68
FRA				5JRQ44	55	- 80	3JRQ55	56	- 68			
FZR	6JRQ12	55	-69	5JRQ22	55	- 64	3JRQ57	45	- 54	3JRQ57	68	- 47
IWM	6JRQ43	55	-63	5JRQ21	56	- 76						
HUN	6JRQ33	55	-83	5JRQ23	55	- 63						
JAP	6JRQ51	61	-73	5JRQ44	52	- 50	3JRQ	66	- 79			
KOR	5JRQ25	55	-65	5JRQ15	55	- 67						
ECN				5JRQ31	56	- 53						
ROM	6JRQ22	55	-66	5JRQ32	55	- 69						
PRO	6JRQ44	55	-74									
KUR	5JRQ33	55	-62	5JRQ33	65	- 81						
ESP	6JRQ34	55	-71		56	- 70	3JRQ71	56	- 50			
USE	5JRQ45	55	-77	5JRQ45	56	- 77						
USI	**5JRQ45**	55	-100	5JRQ45	56	- 76						
USO	6JRQ13	55	-71									
UK										3JRQ52	70	-59
Mean Fit	**6JRQ only**		**-66**	**5JRQ**		**-71**	**3JRQ**		**- 56**	**3JRQ**		**-57**

10.3.1. Effect of test temperature on T_0

The effect of test temperature was also studied within the Fourth CRP, and similar results were obtained as compared with the test results from the Fifth CRP. Results from the Fourth CRP are shown in Figure 10.4, while comparison of both sets of results is shown in Figure 10.5. A similar tendency can be seen in both data sets: a slight tendency for increasing T_0 values with increasing test temperature, but in both cases this effect lays within 90% tolerance bounds and probably is not statistically important.

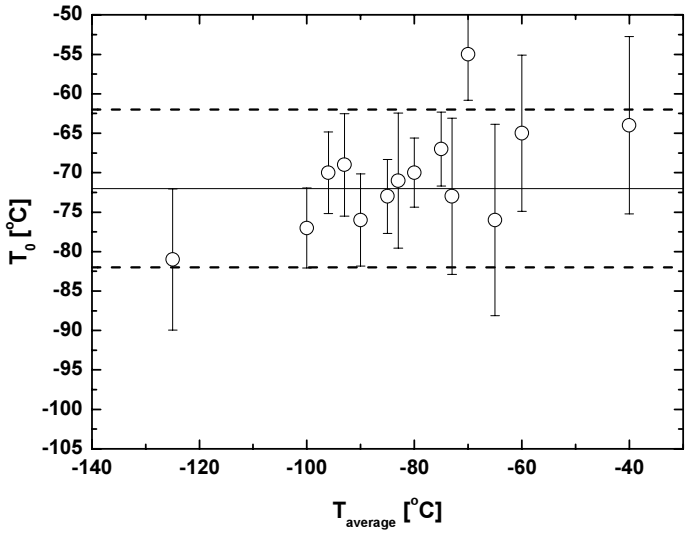

FIG. 10.4 – Effect of Test Temperature on T_0 for Charpy Size SE(B) Specimens in the 5JRQ Plate Section; Error Bars Correspond to Theoretical 90% Confidence Bounds.

10.3.2. Effect of specimen type on temperature T_0

Even though the third and fourth CRPs were not aimed at evaluating fracture toughness specimen type differences, some results were obtained due to different testing possibilities and procedures in individual laboratories, While most laboratories tested Charpy size SE(B) specimens in three-point bending, some laboratories preferred CT specimens. Some laboratories tested both types of specimens.

A comparison of mean values of T_0 determined within all three CRPs is shown in Table 10.3. It is obvious that some bias between values T_0 obtained from specimen types exists; generally, the Charpy size SE(B) specimens give values of more than 10°C lower than CT specimens. The planned experimental results from the Fifth CRP are in good consistency with the previous data, although the results from the Fourth CRP showed the highest bias difference; however, note that both the Third and Fourth CRPs did not have an extensive amount of CT specimen testing and that there were a combination of specimen thicknesses used for the CT testing, while the Fifth CRP utilized 25.4 mm thick CT specimens (1T-CT).

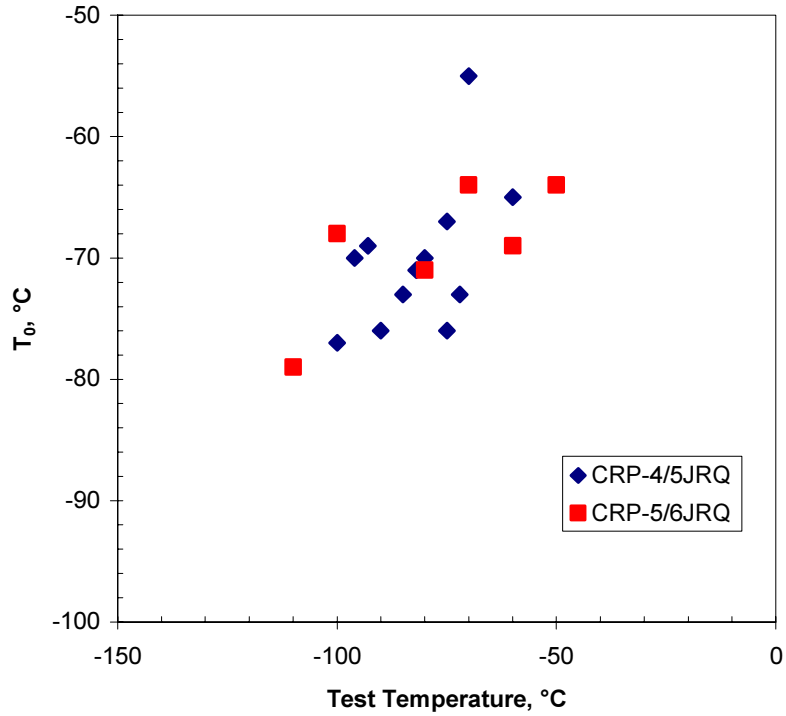

FIG. 10.5 – Comparison of the Effect of Test Temperature on T_0.

Table 10.3 – Comparison of T_0 Values Determined by Charpy Size SE(B) and 1T-CT Specimens (JRQ, T-L Orientation, 55 mm Depth)

Specimen Type	Third CRP	Fourth CRP	Fifth CRP
CT	- 53	- 49	- 54
Charpy Size SE(B)	- 66	- 71	- 66
Specimen Bias	**13**	**22**	**12**

It can be concluded that results obtained within the earlier CRPs are generally consistency with the newest results from this Fifth CRP, even though some of the older data were obtained as a by-product from the more general irradiation experiment design.

11. DISCUSSION AND RECOMMENDATIONS

11.1. CONSEQUENCES FROM THE TEST MATERIALS

In the mandatory part of the Fifth CRP, a large amount of fracture toughness data were produced on a selected material, the IAEA reference steel JRQ, which provides a database suitable for qualification of the Master Curve approach. The JRQ material was selected since this material had been comprehensively characterized in previous CRPs and it is a suitable reactor pressure vessel surveillance reference steel. Also, it was possible to use the some of the same JRQ plate (5JRQ) as in the Fourth CRP to assure comparability of the results of the current and the previous CRPs, in addition to a new JRQ plate (6JRQ).

Secondly, the requirements for testing the JRQ specimens were selected with an aim to minimize all possible effects from the test procedures applied at the different laboratories. It was required that all laboratories perform the tests according to ASTM E 1921-02 to ensure that the results were consistent. Previous experimental data were utilized to assess the temperature dependence of the yield strength (and Young's modulus). Other experimental fracture toughness results were also utilized by some laboratories, and the difference between old and new data evaluated using ASTM E 1921-02 was negligible.

The Master Curve analyses were performed consistently following ASTM E 1921-02 so that no significant deviation should occur from the analysis methods used. The specimens were also machined from the JRQ blocks taking into account the known inhomogeneity of the material in the thickness of the plate, so that through-thickness variation of properties was minimized by primarily using specimens from the ¼-T and ¾-T locations. Some testing was also conducted to include the possibility of non-homogeneity by taking specimens from the ½-T location.

Considering these proactive measures to minimize sources of material variability and experimental and analytical error, the major unspecified factors affecting the scatter of the test data should be limited to:

- Limitations in the test procedures which, despite the standards and recommendations, may lead to variation between the results of different laboratories, and
- Remaining material inhomogeneity which is known to be a potential source of excessive scatter.

It should be recognized that the original measured load-displacement records for individual fracture toughness tests from of each laboratory were not qualified in the re-evaluation performed and presented in this report; therefore, there are some potential issues as to whether all data are proper and reasonable; i.e., meet all of the credibility requirements as stated in ASTM E 1921-02 and as specified for this CRP. As for the 6JRQ plate, the amount of laboratory-specific scatter appears to be smaller than the scatter inherent in the material itself, which is thus anticipated to be the major source of scatter.

The JRQ data produced in this CRP are thus expected to represent a nearly ideal database for characterizing a typical reactor pressure vessel steel with some non-homogeneity. The SINTAP estimates of T_0 (T_0^{SINTAP}) as compared to the ASTM E 1921-02 measures of T_0 confirm, as was anticipated from the results of the previous CRPs, that the material should be regarded as inhomogeneous, even though the estimated values of T_0^{SINTAP} may not in all cases differ much from the ASTM T_0 estimates.

11.2. COMPARISON OF THE MASTER CURVE PREDICTIONS

The uncertainty in T_0 was defined in Equation 7.1 as determined using ASTM E 1921-02. Assuming $\beta = 18^oC$ and the minimum number of specimens (6 valid test results), the value of ΔT_0 is about 11^oC. Correspondingly, with 12 specimens the minimum value is reduced to about 8^oC. Since the T_0 determination is the main source of uncertainty in a Master Curve analysis, one should consider typical scatter in reported T_0 to be $\pm 10^oC$ for the CRP data when 6 to15 specimens have been tested and evaluated. The validity of the Master Curve analyses, which includes considerations such as the shape of the fracture toughness curves or a comparison of individual values of T_0, should be assessed considering this ΔT_0.

In this CRP, the objective was to generate data for assessing factors which might affect the result of a Master Curve analysis and its validity, in particular:

- The test temperature, both in relation to T_0 and the range and number of temperatures (multi vs. single -temperature estimations).
- Macroscopic inhomogeneity of the test material and existence of fracture modes other than pure cleavage.
- The constraint and loading state of different types and sizes of specimens.
- Exceptional material conditions, in general, associated with the factors listed above.

11.3. APPLICABILITY OF THE MASTER CURVE REGARDING THE CURVE SHAPE ASSUMPTION

A basic assumption in the weakest link cleavage fracture model [17] used for the Master Curve is the fixed, empirically determined temperature dependence of fracture toughness, K_{Jc}, which is applied independently of the material. This assumption greatly simplifies the Master Curve method, since only one material-specific parameter, T_0, needs to be determined for a material condition. The benefit is best realized when the model is applied for situations where other characteristic variables may need to be considered. Examples of such situations are the combined estimations of the lower shelf fracture toughness, K_{min}, and T_0 and the irradiation embrittlement parameters and T_0 [18].

The fixed temperature dependence assumption has proven to be reasonable for most structural steels in which fracture exhibits a transition-type behavior and is stress-controlled. Fracture from brittle conditions to high ductility (especially for quenched and tempered structural steels) has been validated for different sizes and types of test specimens [19]. The scope of application also has been extended to different loading rate conditions: dynamic loading and crack arrest [18].

There have, however, been some limited cases where the assumed and measured K_{Jc} versus temperature dependences disagree. In general, such cases have occurred in situations where the basic assumptions of the cleavage fracture model are not fulfilled. For example, a mismatch between the weld and the heat-affected-zone (HAZ) or the base metal properties may lead to a bimodal type temperature dependence of K_{Jc} for the HAZ material, which may be difficult to treat satisfactorily as one population. In these cases, it is more convenient to divide the data statistically into two populations and analyze them separately. The Master Curve, when applied in this manner, allows a separation of different microstructures using suitable criteria, and each “material” can be analyzed to produce a different T_0. This approach has been included using a bimodal Master Curve model, which has recently been developed by Wallin and is an extension of the basic model for analyzing inhomogeneous materials.

11.4. SINGLE- vs. MULTI–TEMPERATURE MODELS FOR ESTIMATING T_0

ASTM E 1921-02 allows use of both the single and multi-temperature models for estimating the value of T_0. The single-temperature procedure is applicable for fracture toughness data measured at only one temperature. Its benefit is that the T_0 can be solved in a closed form, i.e. without iteration. The multi-temperature model is usable for all applicable cases, independently of test temperatures, but the T_0 only can be solved iteratively. The

difference between the T_0 estimates from these solutions has been shown to be negligible. The results generated for the 6JRQ plate support this conclusion.

11.5. SPECIMEN SIZE EFFECT

Specimen size effect is an essential element with fracture mechanics testing in the ductile-to-brittle transition region. The size of a specimen or component affects the measured fracture toughness in two ways: first, there is a statistical effect which is related to the volume of the material and the number of possible cleavage fracture initiators ahead of the crack tip; and second, the size affects the stress state (or the constraint) in the material ahead of the crack tip.

When discussing size effects, one has to distinguish two different cases. The first case consists of loading conditions corresponding to small scale yielding at the crack tip, which is typical of brittle fracture cases with no, or negligible, ductile tearing before cleavage fracture initiation. The second type, which is the more complicated case, is associated with situations when significant ductile tearing occurs prior to the cleavage fracture initiation.

The basic Master Curve model, as described in ASTM E 1921-02, includes the statistical size adjustment, which usually is applied to normalize small specimen K_{Jc} data to a specimen thickness of 25.4 mm (1T). In this adjustment, the K_{Jc} data become "size independent" and, thus, comparable with other data corrected in this same manner. With no, or moderate, ductile tearing this adjustment has proven to be sufficient without any constraint correction. To achieve more accurate and realistic estimates for low constraint geometries, a T_{stress}-based adjustment has been recommended for such structures [20].

11.6. EFFECT OF SPECIMEN TYPE

The two basic specimen types, the compact tension, CT, and the three-point bend single-edge bend, SE(B), specimens are most commonly used in fracture mechanics testing. Due to the different loading geometry, the loading state in these specimens is slightly different. In the CT specimen the stress state in the specimen results from the tensile load and the bending moment, whereas the SE(B) specimen is subjected to a bending moment and some shear contribution.

Both experimental and theoretical investigations have shown that there exists a slight, on the average approximately 8°C, difference in the T_0 values measured with the CT and SE(B) specimens such that CT specimens tend to give higher values of T_0 [21]. This 8°C difference is due to about 1–2°C from the η-factor used in the plastic J-determination is ASTM E 1921-02 and the rest from the loading differences. Compared to the uncertainty of the T_0 determination, this loading rate effect is comparable and also may overlap the uncertainty in T_0, ΔT_0. For this reason, ASTM E 1921-02 has been slow to recommend that this difference be taken into account in the T_0 determination. It is, however, a real effect and amounts to a measured 12°C for the 6JRQ plate.

11.7. ASSESSMENT OF THE 6JRQ PLATE DATA

The JRQ reference material characterized in the Fifth CRP exemplifies a typical quenched and tempered, as-received reactor pressure vessel steel. The previous investigations performed on this material provided a basis to estimate the expectable T_0 value beforehand and to select proper test temperatures around the projected T_0 value. Also, it was known from

the previous studies that some material inhomogeneity existed through the thickness, which also is evident in the measured T_0 values (see Figure 5.2). Therefore, specimens were generally limited to only the ¼-T and ¾-T locations when specimens were fabricated.

Considering the numerous Master Curve analyses performed for a variety of JRQ-type steels elsewhere, it was unlikely that new features not known beforehand would arise. Also, there was no expectation that any abnormal, or exceptional results, would be identified that would give rise for new recommendations for applying the method. The following aspects are, however, emphasized based on the results from this CRP.

11.7.1. Material inhomogeneity

Due to the known inhomogeneity of the test JRQ material, all data were analyzed using both the standard ASTM E 1921-02 procedure and the SINTAP procedure [16]. The results show (Tables 7.1–7.4) that in several test series the difference between the standard T_0 and the SINTAP procedures (T_0-T_0^{SINTAP}) is significant (greater than about 10°C), which confirms that the material can show inhomogeneity. Most of the apparent inhomogeneity can be taken into account by using the higher value of T_0^{SINTAP} for a conservative estimate.

11.7.2. Effect of test temperature on T_0

ASTM E 1921-02 includes a procedure for taking into account the temperature difference between test temperatures and T_0 (T-T_0) on the uncertainty of the T_0 (ΔT_0). According to this procedure, the uncertainty is gradually increased with the temperature difference T-T_0 within the specified range of validity ($-50^oC < T-T_0 < +50^oC$).

The JRQ material was tested at several laboratories using different test temperatures so that either the single- or multi-temperature estimations could be applied for the T_0 determination. These data were thus available also for analyzing the variation of T_0 as a function of test temperature. The results of these analyses are shown in Figs. 7.7 and 7.10. The results indicate a relatively high variation in the T_0 values measured both with the CT and SE(B) specimens over the whole temperature range, i.e., with no clear dependence of T_0 on test temperature. For the SE(B) specimens, the scatter (standard deviation of 11°C) is moderate and in accordance with the uncertainty of T_0 determination (ΔT_0), but the larger scatter obtained for CT specimens (standard deviation of 14°C) exceeds that expected for the material from the ΔT_0 values.

The reason for this large variation may result, for example, from the test methods used by different laboratories or the test material and the variation of its properties. Further analyses of the true reasons may be possible from the original test data, but the performance of these analyses is outside the scope of the CRP. The sources for the larger than expected scatter in the reported T_0 values are not known.

11.7.3. Bias in the T_0 from specimen types

A comparison of the mean T_0 values measured during this CRP supports the results from previous investigations on the expectable bias between the CT and SE(B) specimen types. The mean T_0 measured with the CT specimens was –54°C and that measured with the SE(B) specimens was –66°C (see Figure 7.9 and 7.6, respectively). The difference between the CT and 3PB specimen data is 12°C, which is near expectations.

11.7.4. General comparison of the fifth CRP data

The test data measured by different laboratories are generally consistent using the Master Curve prediction method as evidenced in Section 7 for the JRQ steel. The variation in both the K_{Jc} and T_0 values are however in some ¼-T and ¾-T thickness data larger than the inherent variation of fracture toughness.

In order to clarify all reasons for this variation and, in particular, the role of test methods used by different laboratories, further analyses would require review and use of the original test data from the laboratories. As far as such qualification of data is missing and the true sources for the large scatter in the reported K_{Jc} and T_0 values are not known, the JRQ data only should be used provisionally for other than qualitative recommendations.

In general, the test data of the Fifth CRP and the values of T_0 revealed no key discrepancies with respect to ASTM E 1921-02 procedures which would give rise to recommendations to change the standard. The issue of specimen type bias has recently been added to ASTM E 1921-02, and a reduction in the loading rate requirements is being processed. All basic procedures specified in ASTM E 1921-02 appear to be adequate for the range of variables studied in this CRP, including: (1) specimen size adjustment, (2) data censoring, (3) temperature dependence on the shape of the Master Curve, (4) general validity of the multi-temperature procedure and its consistency with the single-temperature method, (5) the criteria for estimating validity of test data, and (6) the uncertainty of T_0 determination. The analyzed JRQ data illustrate that a bias exists between CT and SE(B) specimens so that the CT specimens give slightly, around 12°C, more conservative estimates for T_0.

12. CONCLUSIONS

The overall results from this CRP provide data which are applicable for both material characterization purposes and test and analysis method development and verification. In general, the results for the JRQ plates and the national materials are consistent with previous data analyzed using ASTM E 1921-02 or its preceding versions or the SINTAP Master Curve procedures.

The following conclusions can be made derived from the JRQ and national material fracture toughness test data analyzed in this CRP:

- The mean fracture toughness of the 6JRQ plate material generally can be described satisfactorily with the standard Master Curve method from ASTM E 1921-02. For conservative estimates, the SINTAP procedure is recommended to be used for materials showing marked inhomogeneity.

- The SINTAP analyses confirm that the 6JRQ plate material can show some weak inhomogeneity; this inhomogeneity can be taken into account by applying the SINTAP procedure for a conservative Master Curve estimate of T_0.

- The overall mean T_0 values show, in accordance with previous investigations, that a bias of around 10°C exists between the T_0 values of CT and SE(B) specimen types with the CT specimens giving higher values of T_0.

- The analyses of both the JRQ and the national materials confirm that the procedures specified in ASTM E 1921-02 as well as the SINTAP procedure are generally valid and applicable for characterizing JRQ type steels and even steels showing distributed inhomogeneity.

- As a general recommendation for further research, the Master Curve based approach, which is mostly applicable in the basic, standard form, should be expanded further to a more generic form which includes procedures for testing the quality of data and special tools for analyzing abnormal cases. These cases may be applicable to materials showing a bimodal type fracture behavior, materials requiring a lower-shelf adjustment, or situations where specific constraint consideration is needed.

APPENDIX. PARTICIPANTS IN THE COORDINATED RESEARCH PROJECT

Country	Institution	Participant
Argentina	Comisión Nacional de Energía Atómica	A. F. Iorio E. Chomik
Brazil	CNEN/CDTN	R. DiLorenzo
Bulgaria	Institute of Metal Science	S. Vodjenicharov
Czech Republic	Nuclear Research Institute Rež	M. Brumovsky M. Kytka
Czech Republic	Vitkovice Research and Development Ltd	K. Matocha
Finland	VTT Industrial Systems	K. Wallin T. Planman
Germany	Forschungszentrum Rossendorf e.V.	H.-W. Viehrig
Germany	Fraunhofer Institut fuer Werkstoffmechanik	D. Siegele
Hungary	Atomic Energy Research Institute	F. Gillemot M. Horvath
Japan	Japan Atomic Energy Research Institute	K. Onizawa
Korea, R6epublic of	Korea Atomic Energy Research Institute	B.S. Lee
Mexico	Instituto Nacional de Investigaciones Nucleares	R.H. Callejas
Romania	Metallurgical Research Institute	N. Lascu
Russian Federation	Russian Research Center “Kurchatov Institute”	A. Kryukov A. Chernobaeva
Russian Federation	Prometey Institute	V.A. Nikolaev
Slovakia	VUJE	L. Kupca
Spain	CIEMAT	J. Lapena M. Serrano
United States of America	Oak Ridge National Laboratory	R. Nanstad
United States of America	ATI CONSULTING	W.L. Server
United states of America	EPRI	S. Rosinsky
EU	Institute for Energy JRC	F. Sevini L. Debarberis
IAEA	Scientific Secretaries	V. Lyssakov K.-S. Kang

REFERENCES

[1] WALLIN, K., "The Scatter in K_{Ic} results," Engineering Fracture Mechanics, Vol. 19, (1984) 1085-1093.

[2] AMERICAN SOCIETY FOR TESTING AND MATERIALS, Test Method for Determination of Reference Temperature, T_0, for Ferritic Steels in the Transition Range, ASTM, West Conshohocken, PA, Vol. 03.01, ASTM E 1921 (2002).

[3] SERVER, W.L., et al., "Application of master curve fracture toughness for reactor pressure vessel integrity assessment in the USA", presented at IAEA Specialists Meeting, Gloucester, UK, 2001.

[4] AMERICAN SOCIETY OF MECHANICAL ENGINEERS, Boiler and Pressure Vessel Code Case N-629, Use of Fracture Toughness Test Data to Establish Reference Temperature for Pressure Retaining Materials, Section XI, Division 1, ASME (1999).

[5] INTERNATIONAL ATOMIC ENERGY AGENCY, Co-ordinated Research Programme on Irradiation Embrittlement of Pressure Vessel Steels, IAEA-176, Vienna (1975).

[6] INTERNATIONAL ATOMIC ENERGY AGENCY, Analysis of the Behaviour of Advanced Pressure Vessel Steels under Neutron Irradiation, Technical Reports Series No. 265, IAEA, Vienna (1986).

[7] INTERNATIONAL ATOMIC ENERGY AGENCY, Reference Manual on the IAEA JRQ Correlation Monitor Steel for Irradiation Damage Studies, IAEA-TECDOC-1230, Vienna (2001).

[8] INTERNATIONAL ATOMIC ENERGY AGENCY, Assuring Structural Integrity of Reactor Pressure Vessels, Vienna (in preparation).

[9] INTERNATIONAL ATOMIC ENERGY AGENCY, Guidelines for Application of the Master Curve Approach to Reactor Pressure Vessel Integrity, Technical Reports Series No. 429, IAEA, Vienna (2005).

[10] DAVIES, L.M., GILLEMOT, F., LYSSAKOV, V., The IAEA International Database on Nuclear Power Plant Life Management, Plant Life Extension (PLEX) Meeting, Prague (1997).

[11] DAVIES, L.M., GILLEMOT, F., LYSSAKOV, V., "The IRPVM Database," IAEA Specialist Meeting "Methodology for Pressurized Thermal Shock Evaluation," Esztergom, Hungary 1997.

[12] VIEHRIG, H.-W., BOEHMERT, J., DZUGAN, J., "Some Issues by Using the Master Curve Concept", Nuclear Engineering and Design, Vol. 212 (2002) 115-124.

[13] MUELLER, G., Investigations on the Segregations and Toughness Properties of the A533B Cl.1 Type IAEA Reference RPV Steel 5JRQ22, Internal Report FZR/FWSM-01 (2000).

[14] AMERICAN SOCIETY FOR TESTING AND MATERIALS, Test Method for Plane-Strain Fracture Toughness of Metallic Materials, ASTM, West Conshohocken, PA, Vol. 03.01 (1997).

[15] WALLIN, K., Use and Application of the Master Curve for Determining Fracture Toughness, VTT, Helsinki (2002).

[16] NEVASMAA, P., BANNISTER, A., WALLIN, K., "Fracture Toughness Estimation Methodology in the SINTAP Procedure," 17th International Conference on Offshore Mechanics and Arctic Engineering, ASME (1998).

[17] WALLIN, K., "Validity of Small Specimen Fracture Toughness Estimates Neglecting Constraint Corrections," Constraint Effects in Fracture: Theory and Applications, ASTM STP 1244, Mark Kirk and Ad Bakker, Eds., American Society for Testing and Materials, Philadelphia (1995) 519537.

[18] WALLIN, K., “Effect of Strain Rate on the Fracture Toughness Reference Temperature T_0 for Ferritic Steels,” Proceedings of Recent Advances in Fracture, Orlando, Florida, (1997) 171182.
[19] WALLIN, K., “Master Curve Analysis of Ductile to Brittle Transition Region Fracture Toughness Round Robin Data,” VTT Publications 367, Technical Research Centre of Finland, Espoo (1998).
[20] WALLIN, K., “Quantifying T_{stress} Controlled Constraint by the Master Curve Transition Temperature T_0,” Engineering Fracture Mechanics, Vol. 68, No. 3 (2001) 303328.
[21] WALLIN, K., PLANMAN, T., VALO, M. and RINTAMAA, R., “Applicability of Miniature Size Bend Specimens to Determine the Master Curve Reference Temperature $T_{0,}$” Engineering Fracture Mechanics, Vol. 68 (2001) 12651296.

ABBREVIATIONS AND SYMBOLS

ΔRT	irradiation-induced shift of Charpy or fracture toughness, °C
ΔT_{41J}	shift in Charpy 41 J transition temperature, °C
ΔT_{100}	shift of the reference fracture toughness temperature at 100 MPa√m, °C
ΔT_{CVN}	Charpy transition temperature shift, °C
ΔT_o	shift of the Master Curve reference temperature, °C
ART	adjusted reference temperature
B_{1T}	thickness B = 1T (25.4 mm)
B_O	thickness of the tested specimen (side grooves are not considered), mm
E	Young's modulus, GPa
E > 0.5 MeV	neutron energies greater than 0.5 MeV
E > 1 MeV	neutron energies greater than 1 MeV
EOL	end-of-life
HAZ	heat-affected-zone near the weld
HSST	heavy section steel technology
JRQ	Japanese reference quality
K_I	applied stress intensity factor, $MPa.m^{0.5}$
K_{Ia}	crack arrest fracture toughness, $MPa.m^{0.5}$
K_{IC}	plane strain crack initiation reference fracture toughness, $MPa.m^{0.5}$
K_{IR}	crack arrest reference fracture toughness, $MPa.m^{0.5}$
K_{Jc}	plain strain cleavage fracture toughness, $MPa.m^{0.5}$
$K_{Jc(0..xx)}$	lower and upper tolerance bound for the estimated fracture toughness, $MPa.m^{0.5}$
$K_{Jc(limit)}$	the validity limit for measured K_{Jc}, $MPa.m^{0.5}$
K_{min}	lower bound fracture toughness fixed at 20 $MPa.m^{0.5}$ in ASTM E 1921-02
NDE	non-destructive examination
PT	pressure-temperature limits
PTS	pressurized thermal shock
RT_{NDT}	reference transition temperature, °C, per ASME Code
RT_{T0}	reference transition temperature based on Master Curve, °C
$RT_{T0(I)}$	initial reference temperature RT_{T0}, °C
SM	sample material
T_{41J}	transition temperature measured at Charpy energy of 41J, °C
T_{CVN}	Charpy V-notch transition temperature corresponding to a 28 J or 41 J Charpy V-notch impact energy, °C
T_F	final transition temperature for WWER RPVs, °C
T_k	transition temperature based on Charpy tests for WWER reactors, °C
T_{k0}	initial transition temperature based on Charpy tests for WWER reactors, °C
T_k^a	maximum allowable transition temperature of WWER RPVs during PTS, °C
T_0	Master Curve reference temperature, °C, per ASTM E 1921

CONTRIBUTORS TO DRAFTING AND REVIEW

Brumovský, M.	Nuclear Research Institute Rež	Czech Republic
Faidy, C.	Electricité de France	France
Planman, T.	VTT Industrial Systems	Finland
Viehrig, H.-W.	Forschungszentrum Rossendorf e.V.	Germany
Kang, K.-S.	International Atomic Energy Agency	
Karzov, G.	Prometey	Russian Federation
Kryukov, A.	Kurchatov Institute	Russian Federation
Lapeña, J.	Centro de Investigaciones Energéticas, Medioambientalesy Tecnológicas	Spain
Lott, R.	Westinghouse	USA
Lyssakov, V.N.	International Atomic Energy Agency	
Nanstad, R.	Oak Ridge National Laboratory	USA
Rosinski, S.	Electric Power Research Institute	USA
Serrano, M.	Centro de Investigaciones Energéticas, Medioambientalesy Tecnológicas	Spain
Server, W.	Advanced Technology Innovation Consulting	USA
Sevini, F.	Institute for Energy JRC	Netherlands

RESEARCH COORDINATION MEETINGS

Vienna, Austria: 19–21 June 2000, 24–26 February 2003,
Prague, Czech Republic: 12–14 2001

CONSULTANT MEETING

Vienna, Austria: 17–19 March 2004